VTT PUBLICATIONS 453

Single phase earth faults in high impedance grounded networks

Characteristics, indication and location

Seppo Hänninen

VTT Energy

Dissertation for the degree of Doctor of Technology to be presented with due permission for public examination and debate in Auditorium S5 at Helsinki University of Technology (Espoo, Finland) on the 17th of December, 2001, at 12 o'clock noon.

TECHNICAL RESEARCH CENTRE OF FINLAND
ESPOO 2001

ISBN 951–38–5960–6 (soft back ed.)
ISSN 1235–0621 (soft back ed.)

ISBN 951–38–5961–4 (URL: http://www.inf.vtt.fi/pdf/)
ISSN 1455–0849 (URL: http://www.inf.vtt.fi/pdf/)

Copyright © Valtion teknillinen tutkimuskeskus (VTT) 2000

JULKAISIJA – UTGIVARE – PUBLISHER

Valtion teknillinen tutkimuskeskus (VTT), Vuorimiehentie 5, PL 2000, 02044 VTT
puh. vaihde (09) 4561, faksi (09) 456 4374

Statens tekniska forskningscentral (VTT), Bergsmansvägen 5, PB 2000, 02044 VTT
tel. växel (09) 4561, fax (09) 456 4374

Technical Research Centre of Finland (VTT), Vuorimiehentie 5, P.O.Box 2000, FIN–02044 VTT, Finland
phone internat. + 358 9 4561, fax + 358 9 456 4374

VTT Energia, Energiajärjestelmät, Tekniikantie 4 C, PL 1606, 02044 VTT
puh. vaihde (09) 4561, faksi (09) 456 6538

VTT Energi, Energisystem, Teknikvägen 4 C, PB 1606, 02044 VTT
tel. växel (09) 4561, fax (09) 456 6538

VTT Energy, Energy Systems, Tekniikantie 4 C, P.O.Box 1606, FIN–02044 VTT, Finland
phone internat. + 358 9 4561, fax + 358 9 456 6538

Technical editing Maini Manninen

Otamedia Oy, Espoo 2001

Hänninen, Seppo. Single phase earth faults in high impedance grounded netwotrks. Characteristics, indication and location. Espoo 2001. Technical Research Centre of Finland, VTT Publications 453. 78 p. + app. 61 p.

Keywords power distribution, distribution networks, earth faults, detection, positioning, fault resistance, arching, neutral voltage, residual current, transients

Abstract

The subject of this thesis is the single phase earth fault in medium voltage distribution networks that are high impedance grounded. Networks are normally radially operated but partially meshed. First, the basic properties of high impedance grounded networks are discussed. Following this, the characteristics of earth faults in distribution networks are determined based on real case recordings. Exploiting these characteristics, new applications for earth fault indication and location are then developed.

The characteristics discussed are the clearing of earth faults, arc extinction, arcing faults, fault resistances and transients. Arcing faults made up at least half of all the disturbances, and they were especially predominant in the unearthed network. In the case of arcing faults, typical fault durations are outlined, and the overvoltages measured in different systems are analysed. In the unearthed systems, the maximum currents that allowed for autoextinction were small. Transients appeared in nearly all fault occurrences that caused the action of the circuit breaker. Fault resistances fell into two major categories, one where the fault resistances were below a few hundred ohms and the other where they were of the order of thousands of ohms.

Some faults can evolve gradually, for example faults caused by broken pin insulators, snow burden, downed conductor or tree contact. Using a novel application based on the neutral voltage and residual current analysis with the probabilistic method, it is possible to detect and locate resistive earth faults up to a resistance of 220 kΩ.

The main results were also to develop new applications of the transient based differential equation, wavelet and neural network methods for fault distance estimation. The performance of the artificial neural network methods was

comparable to that of the conventional algorithms. It was also shown that the neural network, trained by the harmonic components of the neutral voltage transients, is applicable for earth fault distance computation. The benefit of this method is that only one measurement per primary transformer is needed. Regarding only the earth faults with very low fault resistance, the mean error in absolute terms was about 1.0 km for neural network methods and about 2.0 km for the conventional algorithms in staged field tests. The restriction of neural network methods is the huge training process needed because so many different parameters affect the amplitude and frequency of the transient signal. For practical use the conventional methods based on the faulty line impedance calculation proved to be more promising.

Preface

This work is motivated by the practical and theoretical problems studied in several research projects carried out at VTT Energy, and in two technology programmes EDISON and TESLA, during the period 1994–2000.

The work has been supervised by Professor Matti Lehtonen from the Power Systems Laboratory in the Helsinki University of Technology. He has also been the manager of our research group, Electric Energy and IT at VTT Energy, and the leader of the technology programmes EDISON and TESLA. I am deeply grateful to him for the research management, advice, co-operation and support during the academic process.

For practical arrangements and help in organising the field tests and measurements I wish to thank Mr. Veikko Lehesvuo, Mr. Tapio Hakola and Mr. Erkki Antila of ABB Substation Automation Oy. I am also grateful to the distribution companies, who offered the possibility for field tests and measurements in their networks. I am especially indebted to Mr. Jarmo Ström and Mr. Matti Lehtinen of Espoo Electricity, Mr. Stefan Ingman and Mr. Seppo Pajukoski of Vaasa Electricity, Mr. Seppo Riikonen and Mr. Matti Seppänen of North-Karelian Electricity, and both Mr. Arto Järvinen and Mr. Markku Vänskä of Häme Electricity for their assistance in the measurements. I owe special thanks to Miss Gerit Eberl and Professor Peter Schegner from the Dresden University of Technology in Germany, Professor Urho Pulkkinen of VTT Automation and Mr. Reijo Rantanen of Kolster Oy Ab for their co-operation during the work. The financial support of VTT Energy, Tekes National Technology Agency and ABB Substation Automation Oy is also gratefully appreciated. Regarding the English language, I want to thank Mr. John Millar for his good service in checking the manuscript. Many thanks go also to all my superiors and colleagues at VTT Energy for an inspiring work environment.

The warmest thanks I want to address to my wife Eila, my daughters Ulrika and Johanna and my son Heikki. Their support and encouragement made this work possible.

Helsinki, October 2001

Seppo Hänninen

List of publications

This thesis consists of the present summary and the following publications, referred to as Papers A–G:

A Hänninen, S. & Lehtonen, M. 1998. Characteristics of earth faults in electrical distribution networks with high impedance earthing. EPSR (Electric Power Systems Research), Vol. 44, No. 3, pp. 155–161.

B Hänninen, S., Lehtonen, M. & Hakola, T. 2001. Earth faults and related disturbances in distribution networks. Proceedings of IEEE PES SM2001, Vancouver, Canada, July 15–19, 2001. CD-ROM 01CH37262C. 6 p.

C Hänninen, S. & Lehtonen, M. 1999. Method for detection and location of very high resistive earth faults. ETEP (European Transactions on Electrical Power) Vol. 9, No. 5, pp. 285–291. http://www.ETEP.de

D Hänninen, S., Lehtonen, M. & Pulkkinen, U. 2000. A probabilistic method for detection and location of very high resistive earth faults. EPSR (Electric Power Systems Research), Vol. 54, No. 3, pp. 199–206.

E Hänninen, S., Lehtonen, M., Hakola, T. & Rantanen, R. 1999. Comparison of wavelet and differential equation algorithms in earth fault distance computation. PSCC'99. 13th Power Systems Computations Conference, Trondheim, Norway, June 28–July 2, Proceedings Vol. 2. Pp. 801–807.

F Eberl, G., Hänninen, S., Lehtonen, M. & Schegner, P. 2000. Comparison of artificial neural networks and conventional algorithms in ground fault distance computation. Proceedings of IEEE PES WM2000, Singapore, January 23–27, 2000. CD-ROM 00CH37077C. 6 p.

G Hänninen, S. & Lehtonen, M. 2001. Earth fault distance computation with artificial neural network trained by neutral voltage transients. Proceedings of IEEE PES SM2001, Vancouver, Canada, July 15–19, 2001. CD-ROM 01CH37262C. 6 p.

Author's contribution

The author's contribution to the preparation of the publications, which are enclosed as the Appendices A–G, is briefly reviewed in this chapter. The papers summarise the work based on the successive research projects, of which the author as the project manager was in charge. Papers A–B deal with the characteristics of earth faults. The author was responsible for the data acquisition, analyses and the development of the analysis methods.

Papers C–D introduce high impedance earth fault indication and location methods. The author developed the PC based prototype version for the high impedance earth fault indication and location method, based on inventions of professor Lehtonen. The author participated in the development process by verifying the whole system functions on substation level and by testing the method presented in Paper C. The author has developed the probabilistic method for high impedance earth fault location based on Bayesian theorem presented in Paper D.

Papers E–G discuss transient based fault distance computation methods. The author has had the main role in developing the wavelet method and the artificial neural network method based on neutral voltage transient presented in Papers E and G. The neural network application of Paper F was mainly done by Miss Eberl under supervision of Professors Lehtonen and Schegner. In the last mentioned project, the author has participated in guidance of the development work and input data scaling, and the author has done the signal pre-processing.

The author has mainly written Papers A–E and G and he actively participated in the writing of Paper F. Professor Lehtonen has been the supervisor of this work and the co-author of the papers. He also participated in the development of the earth fault indication and location methods. Professor Pulkkinen participated in guidance of the probabilistic approach for fault location in Paper D. Mr. Hakola and Mr. Rantanen arranged and helped in organising the field tests and measurements, which were of vital importance for verification of the fault indication and location methods in Papers B and E.

Contents

List of symbols and notations

ANN	artificial neural network
ATP-EMTP	alternative transients program - electromagnetic transients program
DAR	delayed auto-reclosure
HSAR	high speed auto-reclosure
HV/MV	high voltage/medium voltage
LV	low voltage
L1, L2, L3	phases of the symmetrical three phase system
MEK	mean absolute error
P	permanent fault
RC	remote controlled
SCADA	supervision control and data acquisition
SE	self-extinguished fault
VHF	very high frequency
VLF	very low frequency
1, 2, 0	positive, negative and zero sequence
$\underline{a}$, $\underline{a}^2$	complex rotation operators
C	capacitance
C_e	phase-to-ground capacitance of the unearthed network
C_E	phase-to-ground capacitance of the system
C_{eq}	equivalent capacitance
C_0	zero-sequence capacitance
E	voltage (source), phase voltage
f	frequency
$f(t)$	discrete signal
f_c	charge frequency
f_0	charge frequency for ANN training, fault at the busbar
f'_0	charge frequency of real network, fault at the busbar
f_{30}	charge frequency for ANN training, fault at a distance of 30 km
f'_{30}	charge frequency of real network, fault at a distance of 30 km
$f_0(x)$	current density function of a healthy feeder
$f_1(x)$	current density function of a faulty feeder
$g(t)$	output of the filter

i	integer
$\hat{i}_C$	current transient amplitude
i_k	current sample
I	current
I_{ave}	average value of the compensated feeder currents
$\underline{I}_C$	capacitive current
$\underline{I}_{CE1,CE2,CE3}$	phase to ground capacitive currents
$\underline{I}_e$	earth fault current
$\underline{I}_{ef}$	earth fault current reduced by fault resistance
$\underline{I}_f$	fault current
$\underline{I}_L$	current of the suppression coil
I_{Lmax}	maximum phase current
I_{Lmin}	minimum phase current
$Im[f(t)]$	imaginary part of function
I_{max}	maximum value of the compensated feeder currents
I_{min}	minimum value of the compensated feeder currents
$\underline{I}_P$	current of the parallel resistor
I_w	wavelet coefficient for current
$\underline{I}_{1,2,0}$	positive, negative and zero sequence current
$\Delta\underline{I}_{0i}$	compensated zero sequence current of the feeder i
$\Delta\underline{I}_{0im}$	measured change of zero-sequence current of the feeder i
j	integer
k	integer
l	length
L	inductance
L_{eq}	equvalent inductance
L_T	phase inductance of the substation transformer
$L'_{1,2,0}$	positive, negative and zero sequence inductance
n	integer
$Pr(i\|x)_I$	fault probability by using the point probability method
$Pr(i\|x)_I$	fault probability by using the overall probability method
R	resistance
R_e	earthing resistor
R_f	fault resistance
R_{LE}	phase-to-ground resistance of the system
R_P	parallel resistor

SF	scaling factor
t	time (point)
Δt	sampling period
T	period of the fundamental frequency
U	voltage
U_0	neutral voltage
u_k	voltage sample
$\underline{U}_{L1,L2,L3}$	phase-to-ground voltages
U_w	wavelet coefficient for voltage
$\Delta\underline{U}_{0m}$	measured change of neutral voltage (zero sequence voltage)
$\underline{U}_{1,2,0}$	positive, negative and zero sequence voltages
W_s	wavelet coefficient
$\underline{X}_{1C,2C,0C}$	positive, negative and zero sequence capacitive reactances
$\underline{X}_{1l,2l,0l}$	positive, negative and zero sequence line reactances
$\underline{Z}$	impedance
$\underline{Z}_{1,2,0}$	positive, negative and zero sequence impedances
$\underline{Z}_{0i}$	zero-sequence impedance of the feeder i
$\underline{Z}_e$	earthing impedance
$\underline{Z}_f$	fault impedance
$\underline{Z}_l$	impedance of the line
$\underline{Z}_T$	impedance of the transformer
μ	mean of Normal distribution
μ_0	mean of current distribution in healthy feeders
μ_1	mean of current distribution in faulty feeders
μ_{1C}	mean of current distribution in overall probability method
μ_{1U}	expected fault current in overall probability method
σ	parameter of wavelet function
σ^2	variance of Normal distribution
σ_0^2	healthy feeder current variance in point probability method
σ_{1C}^2	faulty feeder current variance
σ_{1U}^2	expected fault current variance in overall probability method
ω	angular frequency
ω_f	fundamental angular frequency
ω_c	angular frequency of the charge transient
Ψ	wavelet function

1. Introduction

In this thesis, the term high impedance grounding is used to make difference to resistance and solid grounding. In practice this means either ungrounded system where the insulation between neutral and ground is of same order as phase insulation, or compensated neutral system where the neutral point is earthed by suppression coil in order to reduce the fault current. The medium voltage, 20 kV, distribution networks in Finland are mainly of overhead construction with high impedance grounding and are generally radially configured. The networks are operated with an isolated neutral point, but compensation of the earth fault current with the Petersen coil is also used in the substations where a reduction of fault current is needed. While ungrounded systems prevail in the Nordic countries, they are not widely used elsewhere because of the high potential of restriking arcs, which can result in high, destructive transient overvoltages that can be a hazard to equipment and personnel.

The most common fault type in electrical distribution networks is the single phase to earth fault. According to earlier studies, for instance in Nordic countries, about 50–80% of the faults are of this type (Paulasaari et al. 1995, Winter 1988). Earth faults are normally located by splitting the feeder into sections and closing the substation circuit breaker against the fault until the faulty line section is found. The operation of manually controlled switches requires a patrol moving in the terrain. Therefore, to decrease the customer's outage time, the development of indication and location methods for earth faults is essential.

In the past years the indication and location of earth faults have been the object of active study worldwide, and several methodologies have been investigated. On the other hand, numerical relays as part of advanced distribution automation, and modern current and voltage sensors facilitate greater accuracy and selectivity of the protection functions. However, practical implementations of the advanced methods are rare. In comparison to the short circuit fault (Pettissalo et al. 2000), reliable earth fault indicators are lacking, and the fault distance computation is still an open issue for utilities. Therefore, the indication and location methods of earth faults are still in development phase.

With regard to earth fault indication and location, perhaps the most influential factor is the fault resistance. According to our investigations, fault resistances fell into two major categories: one where the fault resistances were below a hundred ohms and the other where they were in the order of thousands of ohms. The last mentioned high impedance disturbances are beyond the reach of protective relays, zero sequence overvoltage relays or overcurrent relays. They are difficult to detect and even if detected, it can be most difficult to discriminate this situation from normal electrical events in the distribution feeders. A fallen or broken distribution conductor can result in a high impedance fault, and it may be a potential hazard if not detected and de-energized.

The difficulty with the accurate location of ground faults in high impedance grounded networks is that the fundamental frequency fault currents are often small compared to the load currents, even in the case of very low fault resistances. The use of fundamental frequency components works only in meshed operation, or when the faulty feeder is possible to connect into a closed ring with one healthy feeder (Winter 1993, Roman & Druml 1999). The utilisation of ground fault initial transients has proved to be the most promising method for the purpose of fault location in radial operation (Schegner 1989, Igel 1990, Lehtonen 1992). However, the practical implementations in relays are restricted, due to the requirement of a sampling rate of 10–20 kHz.

The aim of this study is to determine the characteristics of real earth faults in Finnish network circumstances. Based on these characteristics new methods for high impedance fault indication and location are developed. The contribution of this work is also to study new applications of the transient based differential equation, wavelet and neural network methods for fault distance estimation. The scope is restricted to radially operated systems. In this thesis, the following definitions are used. Low resistance fault means, that the value of fault resistance is 50 Ω or smaller. In the case of a high resistance fault the corresponding value is clearly higher than 50 Ω, typically several thousands of ohms. Fault indication means, that fault is detected somewhere in the distribution network without knowledge of the fault location. Fault location means the determination of the faulty feeder or line section. Fault location is also used as a general term when we are talking about fault distance computation. In fault distance computation, the question is the shortest feeder length from substation to fault point. This does not mean the exact knowledge of fault point,

since if the feeder has many laterals, several possible fault points may be obtained. The actual fault location can be found among these candidate locations by some other means such as by fault indicators or by trial and error.

The work behind this thesis is part of the research work carried out at VTT Energy during the period 1994–2000. The projects belonged to two technology programmes: EDISON on Distribution automation in Finnish utilities (1993–1997) and TESLA on Information technology and electric power systems (1998–2002). This work has been carried out in co-operation with VTT Energy, Helsinki University of Technology, Dresden University of Technology, ABB Substation Automation Oy and various distribution companies. The aim of these projects in the technology programmes was to develop new applications for distribution automation and to decrease outages times.

The thesis is organised as follows. First we discuss the basic properties of the high impedance grounded networks and the calculation of currents and voltages during an earth fault. In chapter 3 the characteristics of the earth faults are analysed based on comprehensive and long-term recordings in real distribution networks. The characteristics discussed can be exploited for high resistance fault indication and location and, in the case of low resistance faults, for fault distance estimation. In chapter 4 the existing methods for the indication and location of high impedance earth faults are reviewed and a novel method, which is based on the analysis of neutral voltage and residual current, is presented. Finally in chapter 5, four different methods are proposed for fault distance estimation in the case of low resistance faults, two of which are based on the line terminal impedance and two on artificial neural networks. The two first mentioned conventional methods have been in pilot use in real network circumstances. The methods are evaluated and compared using real field test data.

The thesis consists of this summary and the original Papers A–G, which are here enclosed as the Appendices A–G.

2. An earth fault in a high impedance grounded network

The way the neutral is connected to the earth determines the behaviour of a power system during a single phase to ground fault. From the safety point of view the earth fault current causes a hazard voltage between the frames of the faulted equipment and earth. In this chapter, the basic properties of unearthed, compensated and high resistance earthed networks are discussed, with special attention given to the calculation of currents and voltages during a fault. Some focus is also given to the fault impedance, which affects the neutral voltage and earth fault current. In Sections 2.6 and 2.7 two important phenomena, the extinction of power arc and earth fault initial transients, are described. The extinction of earth fault arc has a considerable influence to the number of short interruptions to the customers and the initial transients can be utilised for earth fault distance estimation. At the end of this chapter, the measurements are described which were carried out in the distribution utilities in the course of this work.

2.1 Networks with an unearthed neutral

Ungrounded systems have no intentional direct grounding but are grounded by the natural capacitance of the system, see Fig. 1 (Blackburn 1993). The currents of single phase to ground faults are low and depend mostly on the phase to ground capacitances of the lines. The voltage between faulted equipment and earth is small, which improves safety. On the other hand, transient and power-frequency overvoltages can be higher than those obtained, for example, with resistance earthed systems (Lakervi & Holmes 1995). When the fault happens, the capacitance of the faulty phase is bypassed, and the system becomes unsymmetrical. A model for the fault circuit can most easily be developed using Thevenin's theorem. Before the fault, the voltage at the fault location equals the phase voltage E. The other impedances of the network components are small compared to those of the earth capacitances C_e, and can hence be neglected. This leads to the model in Fig. 2.

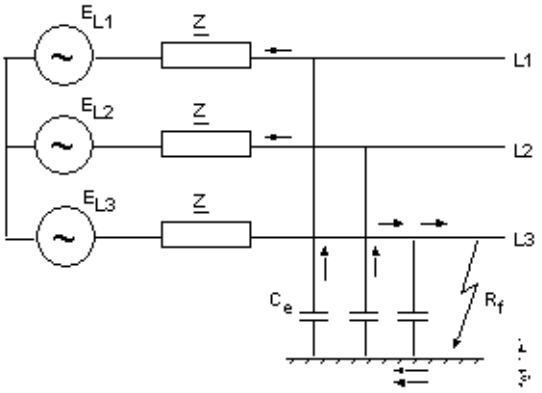

Figure 1. Earth fault in a network with an unearthed neutral (Lehtonen & Hakola 1996).

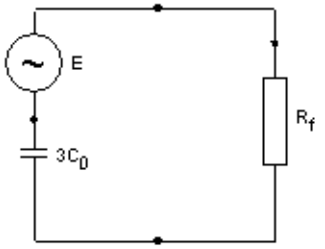

Figure 2. Equivalent circuit for the earth fault in a network with an unearthed neutral (Lehtonen & Hakola 1996).

In the case where the fault resistance is zero, the fault current can be calculated as follows:

$$I_e = 3\omega C_e E \tag{1}$$

where $\omega = 2\pi f$ is the angular frequency of the network. The composite earth capacitance of the network C_e depends on the types and lengths of the lines connected in the same part of the galvanically connected network. In radially operated medium voltage distribution systems this is, in practice, the area supplied by one HV/MV substation transformer.

In earth faults there is usually some fault resistance R_f involved, the effect of which is to reduce the fault current:

$$I_{ef} = \frac{I_e}{\sqrt{1+\left(\frac{I_e}{E}R_f\right)^2}} \tag{2}$$

where I_e is the current obtained from eq. (1). In unearthed systems this does not, in practice, depend on the location of the fault. However, the zero sequence current of the faulty feeder, measured at the substation, includes only that part of the current that flows through the capacitances of the parallel sound lines. This causes problems in the selective location of faults by the protective relaying. The zero sequence voltage U_0 is the same that the fault current causes when flowing through the zero sequence capacitances:

$$U_0 = \frac{1}{3\omega C_0} I_{ef} \tag{3}$$

Using eqs. (1) and (2) this can also be written in the following form:

$$\frac{U_0}{E} = \frac{1}{\sqrt{1+\left(3\omega C_0 R_f\right)^2}} \tag{4}$$

which states, that the highest value of neutral voltage is equal to the phase voltage. This value is reached when the fault resistance is zero. For higher fault resistances, the zero sequence voltage becomes smaller. In the case of a phase to ground fault with zero fault impedance, the unfaulted phase to ground voltages are increased essentially by $\sqrt{3}$ as shown in Fig. 3. Its maximum value is about 1.05U (U = line-to-line voltage) when the fault resistance is about 37% of the impedance consisting of the network earth capacitances. These systems require line voltage insulation between phase and earth (Klockhaus et al. 1981). In a normal balanced system the phase to neutral voltages and phase to ground voltages are essentially the same, but in the case of an earth fault, they are quite different. The neutral shift is equal to the zero sequence voltage. In networks with an unearthed neutral, the behaviour of the neutral voltage during the earth

fault is of extreme importance, since it determines the overall sensitivity of the fault detection.

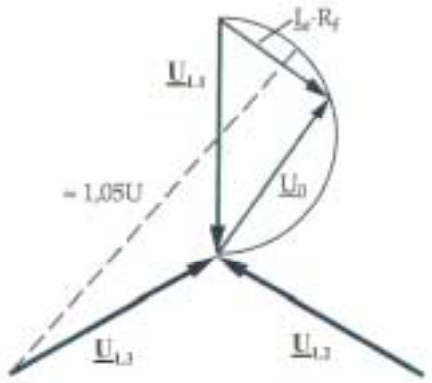

Figure 3. Voltages during an earth fault in an unearthed network (Mörsky 1992).

2.2 Networks with a compensated neutral

The idea of earth fault compensation is to cancel the system earth capacitance by an equal inductance, a so called Petersen coil connected to the neutral, which results in a corresponding decrease in earth fault currents, see Figs 4 and 5. The equivalent circuit for this arrangement is shown in Fig. 6. Instead of one large controlled coil at the HV/MV substation, in rural networks it is possible to place inexpensive small compensation equipment, each comprising a star-point transformer and arc-suppression coil with no automatic control, around the system. With this system the uncompensated residual current remains somewhat higher than in automatically tuned compensation systems (Lakervi & Holmes 1995).

In Fig. 4, the circuit is a parallel resonance circuit and if exactly tuned, the fault current has only a resistive component. This is due to the resistances of the coil and distribution lines together with the system leakage resistances (R_{LE}). Often the earthing equipment is complemented with a parallel resistor R_p, the task of which is to increase the ground fault current in order to make selective relay protection possible.

The resistive current is, in medium voltage networks, typically from 5 to 8% of the system's capacitive current. In totally cabled networks the figure is smaller, about 2 to 3% (Hubensteiner 1989), whereas in networks with overhead lines solely, it can be as high as 15% (Claudelin 1991).

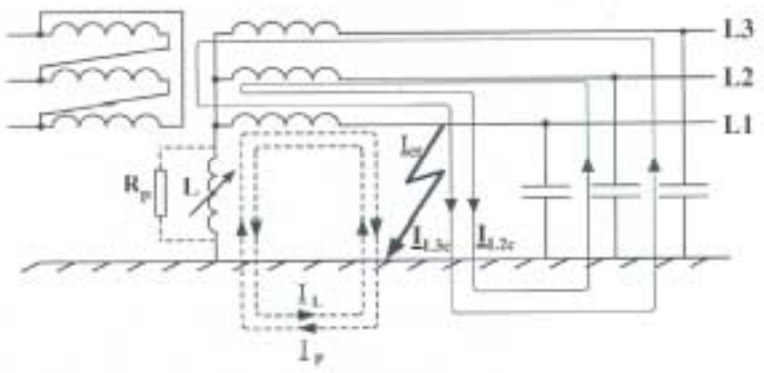

Figure 4. Earth fault in a network with a compensated neutral. $\underline{I}_t=\underline{I}_L-\underline{I}_P$ is the current of the suppression coil and a parallel resistor, $\underline{I}_{L2c}$ and $\underline{I}_{L3c}$ are the capacitive currents of the sound phases, and $\underline{I}_{ef}=\underline{I}_{L2c}+\underline{I}_{L3c}-\underline{I}_t$ is the earth fault current at the fault point (Mörsky 1992).

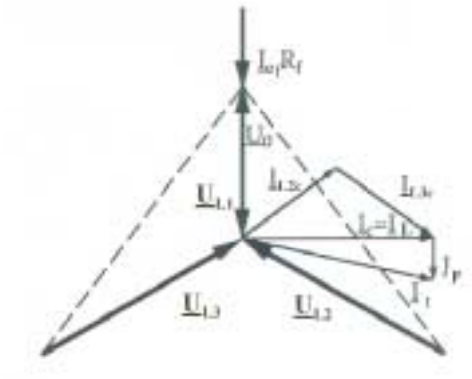

Figure 5. The phasor diagram of currents and voltages in the case of eart fault in fully compensated system. $\underline{I}_C=\underline{I}_{L2c}+\underline{I}_{L3c}$ is the current of earth capacitances, $\underline{I}_t=\underline{I}_L-\underline{I}_P$ is the current of the suppression coil and a parallel resistor, $\underline{I}_{ef}=\underline{I}_c-\underline{I}_t=\underline{I}_P$ is the earth fault current (Mörsky 1992).

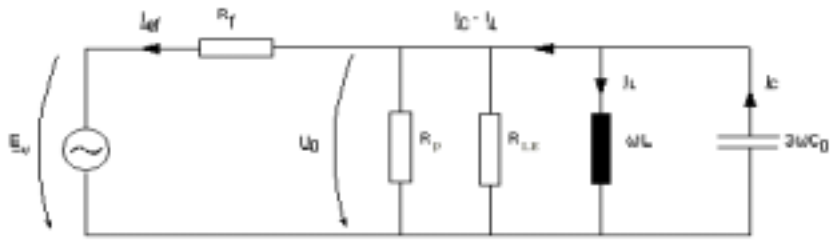

Figure 6. Equivalent circuit for the earth fault in a network with a compensated neutral (Lehtonen & Hakola 1996).

Using the equivalent circuit of Fig. 6, we can write for the fault current:

$$I_{ef} = \frac{E\sqrt{1 + R_{LE}^2\left(3\omega C_0 - \frac{1}{\omega L}\right)^2}}{\sqrt{\left(R_f + R_{LE}\right)^2 + R_f^2 R_{LE}^2\left(3\omega C_0 - \frac{1}{\omega L}\right)^2}}. \tag{5}$$

In the case of complete compensation, the above can be simplified as follows:

$$I_{ef} = \frac{E}{R_{LE} + R_f} \tag{6}$$

The neutral voltage U_0 can be calculated correspondingly:

$$U_0 = \frac{I_{ef}}{\sqrt{\left(\frac{1}{R_{LE}}\right)^2 + \left(3\omega C_0 - \frac{1}{\omega L}\right)^2}} \tag{7}$$

which in the case of complete compensation, is reduced to the following form:

$$\frac{U_0}{E} = \frac{R_{LE}}{R_{LE} + R_f} \tag{8}$$

For the above equations it was assumed that no additional neutral resistor R_p is used. If needed, the effect of R_p can be taken into account by replacing R_{LE} in eqs. (5) to (8) by the parallel coupling of R_{LE} and R_p.

As in the case with an unearthed neutral, the highest zero sequence voltage equals the phase voltage of the system. During earth faults, the neutral voltages are substantially higher in the systems with a compensated neutral than in the case with an unearthed one. Hence a more sensitive indication for high resistance faults can be gained in the former case.

2.3 Networks with high resistance grounding

The grounding resistor may be connected in the neutral of a power transformer or across the broken delta secondary of three phase-to-ground connected distribution transformers. These systems are mainly used in such MV and LV industrial networks, where the continuity of service is important because a single fault does not cause a system outage. If the grounding resistor is selected so that its current is higher than the system capacitive earth fault, then the potential transient overvoltages are limited to 2.5 times the normal crest phase voltage. The limiting factor for the resistance is also the thermal rating of the winding of the transformer.

Earth fault current can be calculated using the equivalent circuit of Fig. 7 as follows:

$$I_{ef} = \frac{E\sqrt{1 + \left(R_e\, 3\omega C_0\right)^2}}{\sqrt{\left(R_f + R_e\right)^2 + \left(R_f R_e\, 3\omega C_0\right)^2}}. \tag{9}$$

When the reactance of the earth capacitance is large compared to the earthing resistance, the above can be simplified as follows:

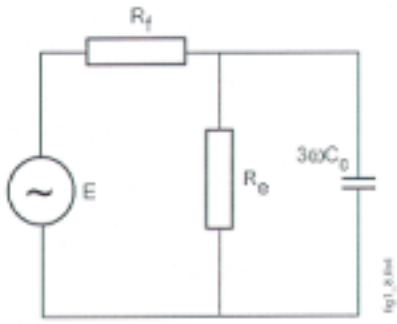

Figure 7. Equivalent circuit for the earth fault in a high-resistance earthed system (Lehtonen & Hakola 1995).

$$I_{ef} = \frac{E}{R_e + R_f} \tag{10}$$

The neutral voltage is

$$U_0 = \frac{I_{ef}}{\sqrt{\left(\frac{1}{R_e}\right)^2 + (3\omega C_0)^2}} \tag{11}$$

The highest neutral voltage in high resistance earthed networks is equal to the phase to ground voltage when the fault resistance is zero. The corresponding phase to ground voltage in two sound phases is equal to the line voltage. Due to the fact that Finnish medium voltage distribution networks are unearthed (80%) or compensated (20%), the high resistance earthed systems are not discussed later in this work (Nikander & Lakervi 1997).

2.4 Sequence network representation

Symmetrical components are often used when analysing unsymmetrical faults in power systems. All cases of neutral earthing, presented in Sections 2.1–2.3, can be analysed using the sequence network model and the appropriate connection of component networks, which depend on the fault type considered. The simplified equations of previous sections can be derived from the general model.

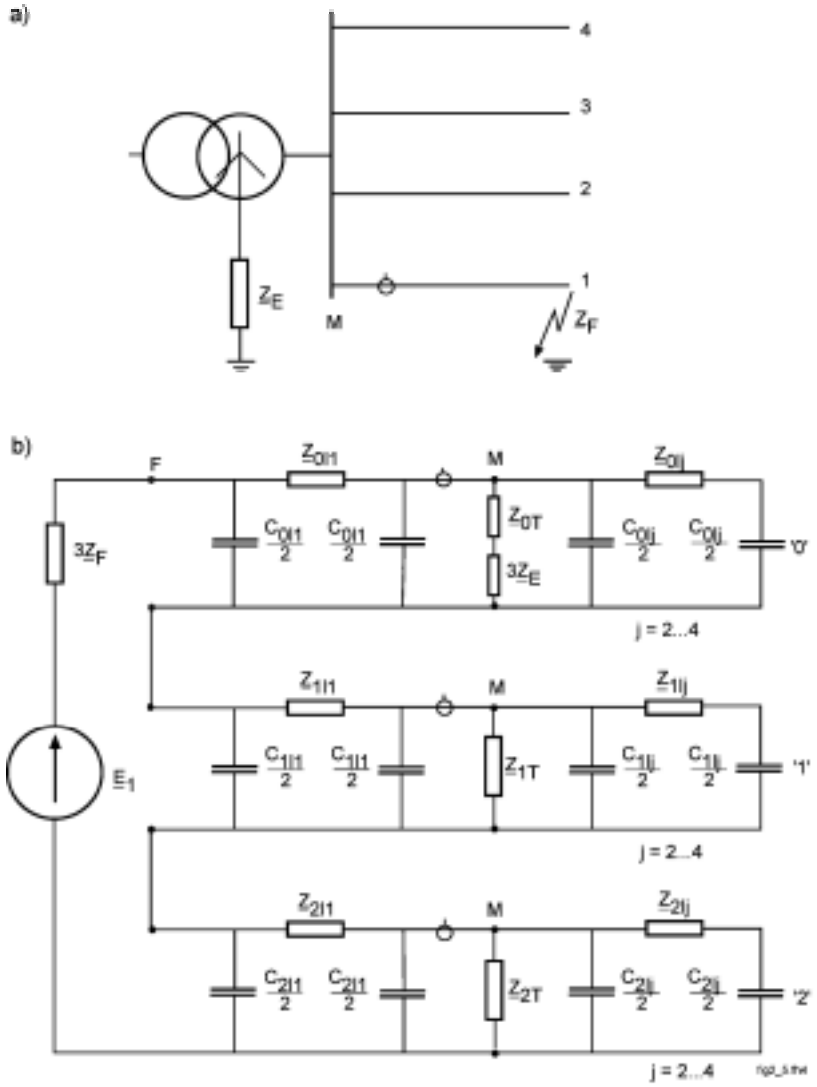

Figure 8. Single phase to earth fault in a distribution network. M is the measurement point, F refers to the fault location. $\underline{Z}_E$ is the earthing impedance and $\underline{Z}_F$ is the fault impedance. a) The network and b) the corresponding symmetrical component equivalent circuit. Z_{0T}, Z_{1T} and Z_{2T} are zero sequence, positive sequence and negative sequence impedances of the substation transformer. j = 2...4 refers to the impedances of the parallel sound lines (Lehtonen & Hakola 1995).

For a phase to ground fault in radial operating system, the sequence networks and their interconnections are shown in Fig. 8. For example in unearthed network $\underline{Z}_E = \propto$ and the distributed capacitive reactances $\underline{X}_{1C}$, $\underline{X}_{2C}$ and $\underline{X}_{0C}$ are very large, while the series reactance (or impedance) values $\underline{Z}_{0l1}$, $\underline{Z}_{1l1}$, $\underline{Z}_{2l1}$, $\underline{Z}_{1T}$, $\underline{Z}_{2T}$, are relatively small. Thus, practically, $\underline{X}_{1C}$ is shorted out by $\underline{Z}_{1T}$ in the positive sequence network, and $\underline{X}_{2C}$ is shorted out by $\underline{Z}_{2T}$ in the negative sequence network. Since these impedances are very low, $\underline{Z}_{1T}$ and $\underline{Z}_{2T}$ approach zero relative to the large value of $\underline{X}_{0C}$. Therefore, the sequence currents can be approximated by the following equation in the case of zero fault resistance (Blackburn 1993).

$$\underline{I}_1 = \underline{I}_2 = \underline{I}_0 = \frac{\underline{E}_1}{\underline{Z}_{1T} + \underline{Z}_{1l1} + \underline{Z}_{2T} + \underline{Z}_{2l1} + \underline{X}_{0C}} \cong \frac{\underline{E}_1}{\underline{X}_{0C}} \tag{12}$$

and

$$\underline{I}_f = 3\underline{I}_0 = \frac{3\underline{E}_1}{\underline{X}_{0C}} \tag{13}$$

The unfaulted phase L2 and L3 currents will be zero when determined from the sequence currents of Eq. 12. This is correct for the fault itself. However, throughout the system the distribution capacitive reactances $\underline{X}_{1C}$ and $\underline{X}_{2C}$ are actually in parallel with the series impedances $\underline{Z}_{1l}$, $\underline{Z}_{1T}$ and $\underline{Z}_{2l}$, $\underline{Z}_{2T}$ so that in the system $\underline{I}_1$ and $\underline{I}_2$ are not quite equal to $\underline{I}_0$. Thus the phase to ground capacitive currents $\underline{I}_{CE2}$ and $\underline{I}_{CE3}$ exist and are necessary as the return paths for the fault current $\underline{I}_f$. When faults occur in different parts of the ungrounded system, $\underline{X}_{0C}$ does not change significantly. Since the series impedances are quite small in comparison, the earth fault current is practically the same and is independent of the fault location. The zero sequence current measured at the substation includes that current flowing in the fault point, less the portion that flows trough the earth capacitances of the faulty line itself, see Fig. 8.

2.5 Fault impedance

Earth faults are seldom solid but involve varying amounts of impedance. However, it is generally assumed in protective relaying and most fault studies that the connection of the phase conductor with the ground involves very low and generally negligible impedance. For the higher voltages of transmission and subtransmission this is true. In distributions systems, however, very large to basically infinite impedances can exist. Many faults are tree contacts, which can be of high impedance, especially in wintertime when the ground is frozen, see Papers A–C. Covered and also bare conductors lying on the ground may or may not result in a significant fault current and can be highly variable. Many tests have been conducted over the years on wet soil, dry soil, rocks, asphalt, concrete and so on, with quite variable and sometimes unpredictable results (see, for example, Sultan et al. 1994, Russell & Benner 1995). Thus in most fault studies, the practice is to assume zero ground impedance for maximum fault current values. In addition, it is usual to assume that the fault impedance is purely resistive.

Fault impedance includes also the resistance of the power arc, which can be approximated by the following formula (Warrington 1962)

$$R = 8750l / \left(0.305 I^{1.4}\right) \tag{14}$$

R is expressed in Ω, l is the length of the arc in meters in still air, and I is the fault current in amperes. Another highly variable factor is the resistance between the line pole or the tower and ground. The general practice is to neglect this in most fault studies, relay applications and relay settings.

2.6 Extinction of earth fault arc

Most earth faults cause an arc in their location. The capacitive fault current is interrupted, either by switchgear or self-extinction of the power arc, at the instantaneous current zero. The factors affecting the power arc extinction in free air are the current magnitude, recovery voltage, time the arc existed, length of the spark gap and wind velocity. The current magnitude and the recovery voltage

are the most important (Poll 1984, Lehtonen & Hakola 1996). As a consequence of the arc extinction the zero sequence system is de-energized and the voltage of the faulted phase is re-established. This causes a voltage transient often called the recovery voltage. The power arc extinction depends on the rising speed of the recovery voltage over the spark gap. The lower steepness of the recovery voltage is the main reason why the possibility of arc extinction with higher current is much greater in a compensated than in an isolated system, see Fig. 9. In compensated network, the arc suppression is very sensitive to the suppression coil tuning. By examining field tests (Poll 1983, Nikander & Lakervi 1997), the compensation degree must be relatively high (about 75%–125%) before the self-extinction of the earth fault arc can be considerably improved. In partially compensated networks with low compensation degree the use of correctly dimensioned additional star point resistor parallel with the coil reduces the steepness and the amplitude of the recovery voltage transient.

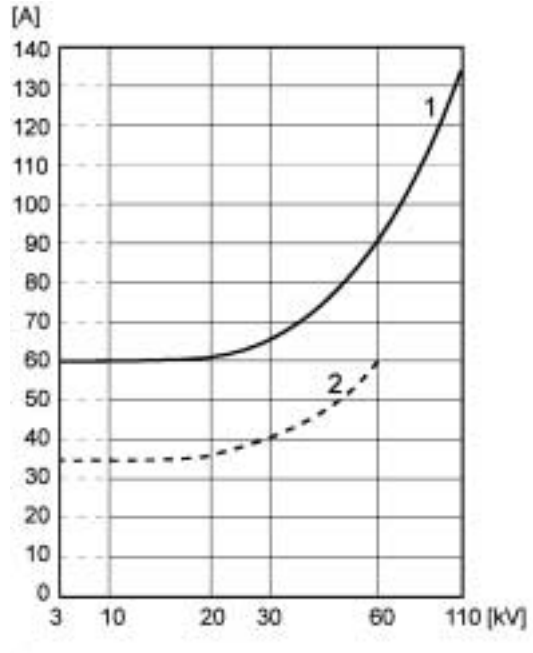

Figure 9. Current limits of earth fault extinction in compensated (1) and unearthed systems (2). Horizontal axis: Nominal voltage. Vertical axis: The residual fault current in a compensated network or the capacitive fault current in an unearthed system (VDE 0228 1987).

According to Fig. 9 the current limits of earth fault extinction are 60 A and 35 A in 20 kV compensated and unearthed systems, respectively. In rural overhead line networks, horn gaps are widely used for the overvoltage protection of small distribution transformers. The power arc is not as free to move as in the case of a flashover of an insulator string for instance. Due to this the above mentioned current limits have been reported to be considerable lower, 20 A and 5A respectively (Taimisto 1993, Haase & Taimisto 1983).

2.7 Transient phenomena in earth fault

Earth fault initial transients have been used for fault distance computation due to the fact, that the transient component can easily be distinguished from the fundamental frequency load currents. It has in many cases higher amplitude than the steady state fault current, see Fig. 10. When an earth fault happens, three different components can be distinguished. The discharge transient is initiated when the voltage of the faulty phase falls and the charge stored in its earth capacitances is removed. Because of the voltage rise of the two sound phases, another component, called charge transient, is created. The interline compensating components equalize the voltages of parallel lines at their substation terminals. In compensated networks there is, in addition, a decaying DC-transient of the suppression coil circuit (Lehtonen 1992). This component is usually at its highest, when the fault takes place close to voltage zero. If the coil is saturated, the current may also include harmonics.

The charge transient component is best suitable for fault location purposes. The charge component has a lower frequency and it dominates the amplitudes of the composite transient. If we suppose, that fault is located at the 110/20 kV substation, the angular frequency of the charge component in the undamped conditions can be calculated as follows (Pundt 1963, Willheim & Waters 1956), see Fig. 11:

$$\omega_c = \frac{1}{\sqrt{L_{eq} C_{eq}}} = \frac{1}{\sqrt{3L_T \left(C + C_E\right)}} \tag{15}$$

where

$$L_{eq} = 1.5 L_T ; \qquad C_{eq} = 2\left(C + C_E\right) \tag{16}$$

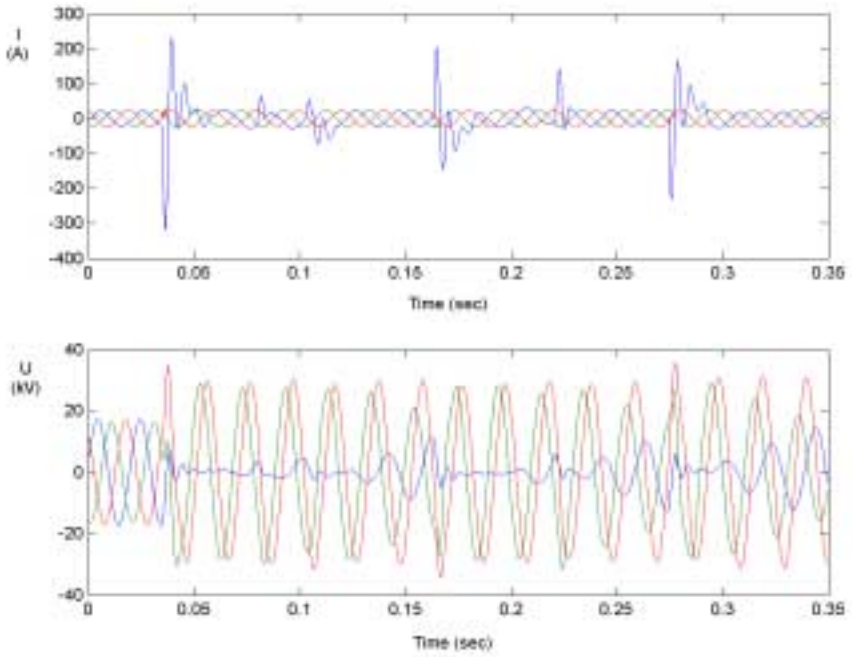

Figure 10. Transient phenomenon in the phase currents (I) and phase voltages (U) recorded in a compensated network.

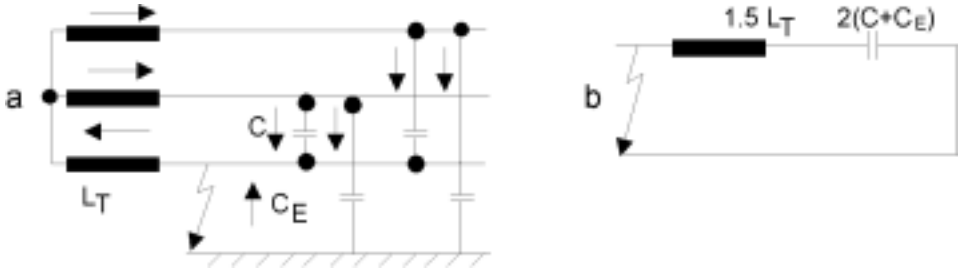

Figure 11. The network model for the charge transient (a) and the corresponding circuit (b).

and where L_T is the substation transformer phase inductance, C is the phase to phase capacitance and C_E is the phase to earth capacitance of the network. If the fault happens at the instantaneous voltage maximum, the transient amplitude is

$$\hat{i}_c = \frac{C_{eq}\omega_c}{3C_E\omega_f} I_e \qquad (17)$$

where ω_f is the fundamental frequency and I_e is the uncompensated steady state earth fault current. The amplitude depends linearly on the frequency ω_c. Since it is not unusual for this to be 5000 rad/s, the maximum amplitudes can be even 10–15 times that of the uncompensated fundamental frequency fault current.

In real systems there is always some damping, which is mostly due to the fault resistance and resistive loads. Damping affects both frequencies and amplitudes of the transients. The critical fault resistance, at which the circuit becomes overdamped, is in overhead line networks typically 50–200 Ω, depending on the size of the network and also on the fault distance. If the resistive part of the load is large, damping is increased, and the critical resistances are shifted into a lower range. Basically the distribution network is a multi-frequency circuit, since every parallel line adds a new pair of characteristic frequencies into the system. These additional components are, however, small in amplitude compared to the main components. According to the real field tests, the amplitudes of charge transients agreed with equation 17 (Lehtonen 1992). In the case of the discharge component the amplitude was typically 5 to 10% of the amplitude of the charge component. The fault initial moment, i.e. the instantaneous value of the phase voltage, affects the amplitude of the transients. However, the faults are more likely to take place close to the instantaneous voltage maximum, when the amplitudes are relatively high. The frequencies varied through a range of 500–2500 Hz and 100–800 Hz for discharge and charge components respectively.

2.8 Measurements in distribution utilities

The characteristics of earth faults were determined based on long-term surveys in real distribution networks. The developed indication and location methods were tested using field test with artificial faults. The methods were also in pilot use in real networks. The measurements were carried out together with VTT, ABB Substation Automation Oy and distribution utilities. ABB Substation Automation Oy supplied the recorder equipment and measuring instruments. The phase currents and voltages were measured from the secondary of the

matching transformers of the protection relays. The zero sequence voltage was measured from the open delta secondary of the three single-phase voltage transformers. In the following, a short summary of the measurements is presented.

Real earth faults were recorded at the Gesterby substation of Espoo Electricity, where the distribution network is isolated, and at the Gerby substation of Vaasa Electricity, where the distribution network is compensated during the years 1994–1996 and 1998–1999. The recorders were triggered if the predetermined threshold value of neutral voltage was exceeded. In the case of fault, phase voltages and currents, neutral voltage and residual currents were measured from the feeders surveyed. In the last mentioned recording project, recorders were additionally triggered regularly at 10-minute intervals, so that the network parameters could be determined also in normal network conditions, see papers A and B. Altogether 732 real disturbances were recorded.

During the years 1995–1996, the developed prototype system for the neutral voltage survey was in test use at the Renko and Lammi substations of Häme Electricity and at the Honkavaara and Kitee substations of North Karelia Electricity. In the former case the neutrals were isolated and in the latter case compensated. The measuring system consisted of the disturbance recorders and PC in the substation with modem connection via telephone network to VTT. Phase voltages of 0.14 sec periods were recorded with 1.5 kHz sampling rate at the one minute interval. The data were analysed at the substation. Together 227 neutral voltage variations were detected. These data were used for development of high resistive earth fault indication methods, see Paper C.

High resistive earth fault field experiments were carried out during the normal network conditions at the Lammi substation of Häme Electricity 14.11.1995 and at the Maalahti substation of Vaasa Electricity 9.5.1996, where the distribution networks are unearthed. Field tests were also carried out at the Kitee substation of North Karelia Electricity 11.9.1996, where the distribution network is compensated. During the tests, fault resistances from 20 to 220 kΩ with 20 kΩ steps were connected to each phase of the three phase systems in turn at a distant line location. At the Lammi substation, so-called tree experiments were also made, where each phase of the line was connected to a growing tree. Simultaneously, the phase voltages, neutral voltage and residual current of faulty

feeder were recorded. At the Kitee substation additionally, the residual currents of five parallel feeders were measured. In the case of Maalahti and Kitee, one phase voltage and phase currents of the faulty line were also measured at one pole-mounted disconnector substation. The test data were recorded using both 1.5 kHz and 10 kHz sampling rate at the Lammi substation. In the other substations, the sampling rate was 500 Hz. The measurements were made with one 8-channel Yokogava measuring instrument and with three 4-channel digital storage oscilloscopes, see Papers C and D.

For testing the fault distance computation algorithms, the same earth fault test data were used as reported in Lehtonen (1992). These field experiments were carried out in South-West Finland Electricity 19.–20.6.1990 where the distribution network is partially compensated, in Vaasa Electricity 11.–12.12.1990 where the distribution network is compensated and in Espoo Electricity 18.–19.12.1990 where the distribution network is unearthed. The same experiments were repeated many times with different fault resistances and line locations. The voltage and current of the faulty phase were measured with 20 kHz sampling rate, see Papers E–G.

3. Characteristics of the earth faults based on the measurements

To develop protection and fault location systems, it is important to obtain real case data from disturbances and faults that have occurred in active distribution networks. In this chapter the characteristics of earth faults are analysed based on comprehensive and long-term recordings. In addition, the characteristics of the faults are discussed which can be exploited for high resistance fault indication and location and, in the case of low resistance faults, for fault distance estimation.

3.1 Fault recording

The characteristics of earth faults and related disturbances were studied by recording disturbances during the years 1994–1996 and 1998–1999 in networks with an unearthed or a compensated neutral. The networks were mainly of overhead construction, with a smaller share of underground cables. The recorders were triggered when the neutral voltage exceeded a threshold value. In the first recording project, see Paper A, due to the size of the sample files and to the slowness of the telecommunication system, the detection sensitivity had to be set relatively low. Therefore, a large part of the high resistance faults was lost. In the second project, see paper B, the current and voltage samples were analysed at the substation immediately after their recording. The sensitivity of the triggering could be increased, resulting in a more comprehensive recording of the high resistance faults.

In the occurrence of disturbances, the traces of phase currents and voltages, and neutral currents and voltages were recorded at the faulted feeder. In what follows, the clearing of earth faults, the relation between short circuits and earth faults, arc extinction, arcing fault characteristics, the appearance of transients, and the magnitudes and evolving of fault resistances are discussed.

3.2 Fault clearing

During the recording projects, altogether 732 real case events were recorded from the feeders under surveillance. The majority of the disturbances disappeared of their own accord without any action from the circuit breaker. If these temporary disturbances were to be excluded, the division of faults into earth faults and short circuits would be about 70% and 30% in the unearthed network, and about 60% and 40% in the compensated network, respectively, see Figs. 12 and 13. This division is dependent on the network circumstances, which were equally divided into fields and forests in the case of the surveyed lines. Paper A shows contrary results acquired from a third power company, where 74% of the faults were short circuits and 26% earth faults. Here the number of faults was acquired with the aid of numerical relays in the substations. The lines were in the majority located in forests, and the period surveyed was about three years. About 82% of the earth faults that demanded the action of a circuit breaker were cleared by auto-reclosing and 17% of the earth faults were permanent. The share among permanent faults was fifty-fifty between earth faults and multiphase faults.

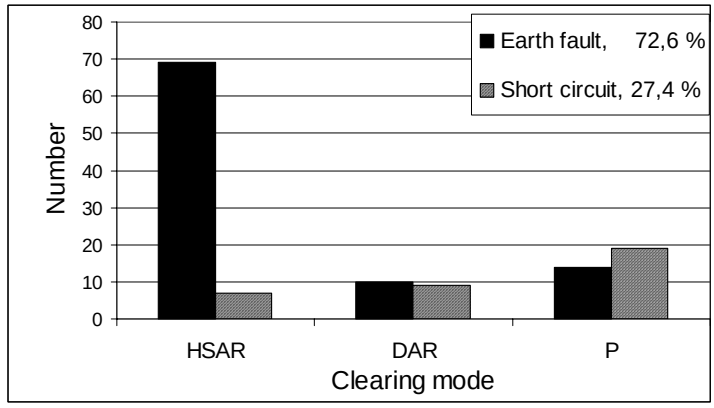

Figure 12. Number of the disturbances classified by means of clearing in the unearthed network (HSAR = high-speed auto-reclosure, DAR = delayed auto-reclosure, P = permanent fault).

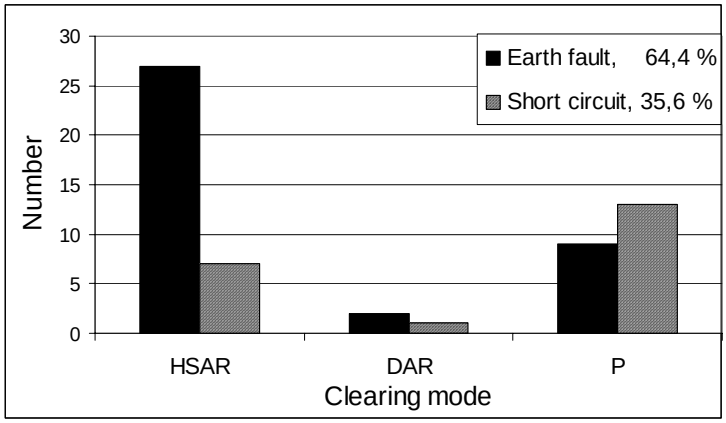

Figure 13. Number of the disturbances classified by means of clearing in the compensated network.

The aforementioned figures are possible to compare to the statistics of the Finnish Electricity Association Sener (2000) concerning only the permanent faults. The outage statistics of Sener cover 83.6% of the feeder length in the medium voltage distribution networks of the whole country. According to these statistics, the share between permanent earth fault and multiphase fault was 46% and 54%, respectively, and taking into account only the regional unearthed networks, 48% and 52%.

3.3 Fault resistances

There are clearly two major categories of earth faults, see Figs 14 and 15. In the first category, the fault resistances are mostly below a few hundred ohms and circuit breaker tripping is required. These faults are most often flash-overs to the grounded parts of the network. Distance computation is possible for these faults. In the other category, the fault resistances are in the order of thousands of ohms. In this case, the neutral potentials are usually so low that continued network operation with a sustained fault is possible. The average time from a fault initiation to the point when the fault resistance reached its minimum value was below one second. The starting point for a disturbance was when the neutral voltage exceeded the triggering level. The disturbances developed very quickly and, as a whole, the fault resistances reached their minimum values in the very

beginning of the disturbances. However, some faults evolve gradually. Paper C shows the computed fault resistances for the real case disturbances which were caused by a broken pin insulator, snow burden, downed conductor, faulty transformer or tree contact. These faults could be detected from the change in neutral voltage many hours before the electric breakdown. The last mentioned results were acquired from a neutral voltage survey at four substations belonging to North-Karelian Electricity and Häme Electricity during the years 1995 and 1996.

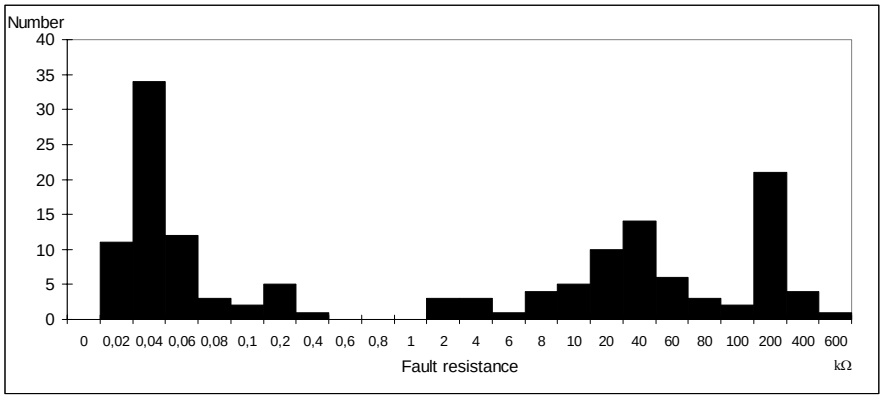

Figure 14. The division of the fault resistances in the unearthed network recorded during the years 1994–1996.

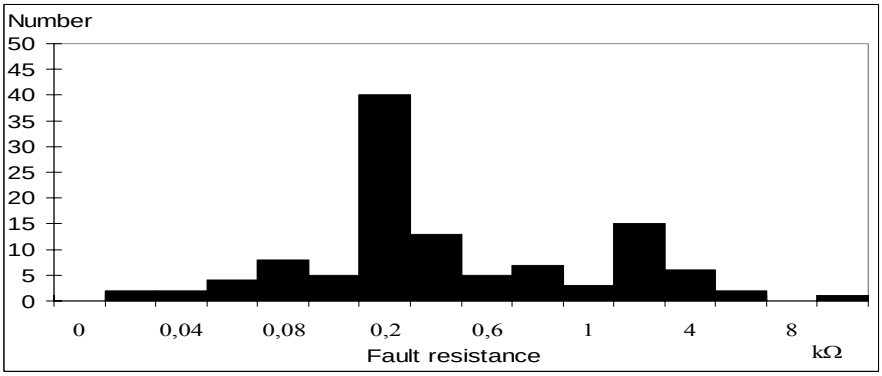

Figure 15. The division of the fault resistances in the compensated network recorded during the years 1994–1996.

3.4 Arcing faults

In an arcing earth fault, the arc disappears at the current zero crossing, but is immediately re-established when the voltage rises. In the isolated neutral network, about 67% of the disturbances were arcing faults. The average duration of the arcing current was approximately 60 ms. In the compensated network, the corresponding figures were 28% and approximately 30 ms. The overvoltages in the unearthed network were higher than in the compensated neutral network, and more than double the normal phase voltage. An arcing fault creates an increase in the harmonic levels of the feeder. In particular, high resistance arcing faults are highly random as viewed from their current waveforms. This is due to the dynamic nature of the unstable interface between the phase conductor and the fault path. Mechanical movement, non-linear impedance of the fault path and arc resistance affect the fault current and make the time domain characteristics of the fault appear to be random, see Fig 16.

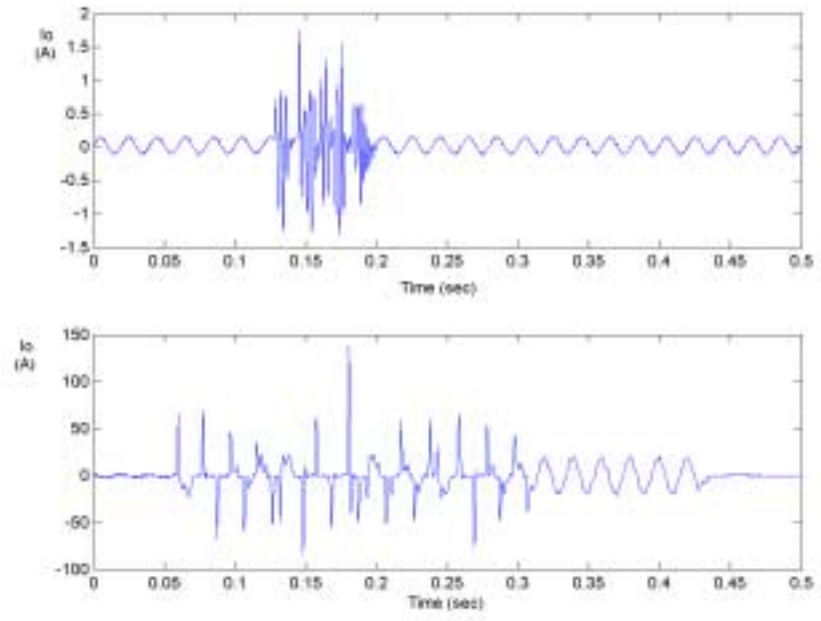

Figure 16. Zero sequence current I_0 during a high resistance arcing fault (upper curve) and during a low resistance arcing fault (lower curve), recorded in the unearthed network.

3.5 Autoextinction

An earth fault arc can extinguish itself without any auto-reclosing function. One indication of autoextinction is subharmonic oscillation in the neutral voltage, showed in Paper B (Poll 1983). This oscillation is due to discharge of the extra voltage in the two sound phase-to-earth capacitances via the inductances of the voltage transformers. In the case of autoextinction, the average and maximum measured residual currents were 0.9 A and 9.5 A in the unearthed network, and 5.7 A and 23.8 A in the compensated network, respectively, see Fig. 17. In unearthed network, 95% of disturbances extinguished in shorter time than 0.3 sec. High resistance faults disappeared noticeably more slowly in the compensated network. About 50% of faults lasted less than 0.5 sec and 80% of the faults less than 1 sec. Especially in the unearthed systems, the maximum currents that allowed for autoextinction were clearly smaller than had previously been believed, see Fig. 9 (Poll 1984). It must be taken into account that, in the unearthed network, surge arresters were used for overvoltage protection, whereas in the compensated neutral system spark gaps were used. The difference to the earlier reported results is that they were determined from artificial earth fault test whereas the results of Fig. 17 were measured from real earth faults.

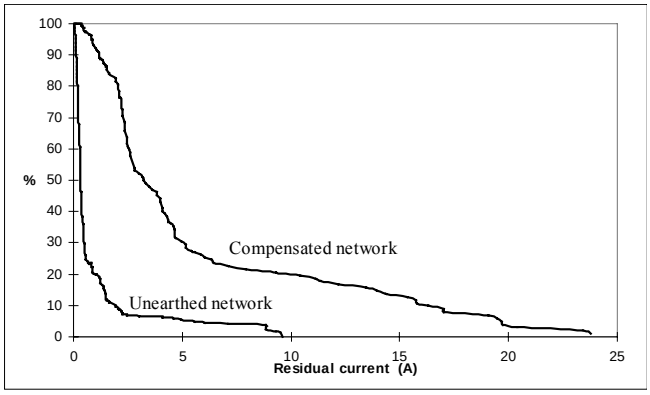

Figure 17. Cumulative characteristic of faults which extinguished themselves versus maximum residual current.

The maximum capacitive earth fault current in the unearthed network under surveillance was either about 70 A or 35 A. This was due to the fact that during the heavy electrical load, the distribution network of the substation was divided

into two calvanically isolated parts. In the compensated network, the maximum earth fault current was about 23 A (with zero fault resistance). The downward slopes of the curves in Fig. 17 may primarily be due to faults to uncontrolled parts of the network, where fault resistance is high and the air gap is smaller than in the case of the faults to grounded parts of the network equipment. The low current values in the case of autoextinction may also be due to the relay settings, which allowed short time only for arc in the case of low resistive faults. The delay of the high-speed autoreclosure was 0.4 s in the unearthed network and 0.6 s in the compensated network. However according to earlier studies, the maximum current for autoextinction, which was measured in real unearthed network, was 5 A (Poll 1984, Haase & Taimisto 1983). According to this study, 95% of earth faults extinguished itself, when the earth fault current was 5 A or lower in the unearthed network.

3.6 Transients

The transient components of the voltages and currents are based on the charging of the capacitances of the two healthy phases and the discharging of the faulted phase's capacitance. Transients could be detected in nearly all fault occurrences that demanded the function of the circuit breaker, see Fig 18. In addition, about 70% of the transients were oscillatory, see Paper A. These characteristics of the transient phenomenon can be made use of in the relay protection systems and in fault location. The fault distance computation using transients was possible in all permanent fault cases. For these, the charge transient frequency varied in the range of 246 Hz to 616 Hz.

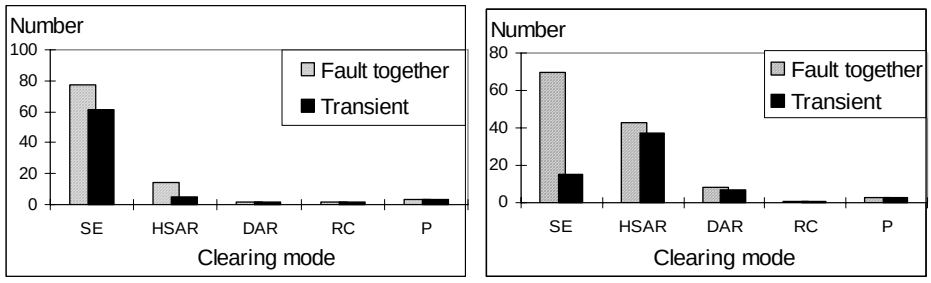

Figure 18. Appreance of transients classified by means of fault clearing in the compensated network (left) and in the unearthed network (right) recorded during the years 1994–1996.

3.7 Discussion of the characteristics

The characteristics were mainly determined for 20 kV networks of overhead construction, with a smaller share of underground cables. In the unearthed network, more than a half of the disturbances were arcing faults. These can lead to overvoltages higher than double the normal phase to ground voltage. Only a few arcing faults occurred in the compensated network. An arcing fault creates an increase in the harmonic levels in the feeder. The performance of the protection relay algorithms is dependent on obtaining accurate estimates of the fundamental frequency components of a signal from a few samples. In the case of an arcing fault, the signal in question is not a pure sinusoid and thus can cause errors in the estimated parameters (Phadke & Thorp 1990). Harmonic content can be exploited for fault indication purposes in high resistance faults.

An earth fault arc can extinguish itself without any auto-reclosing function and interruptions can thus be avoided. Especially in the unearthed systems, the maximum currents that allowed for autoextinction were, in spite of the use of surge arresters, clearly smaller than had previously been believed. Fault resistances fell into two major categories, one where the fault resistances were below a few hundred ohms and the other where they were in the order of thousands of ohms. In the first category, faults are most often flash-overs to the grounded parts of the network. Distance computation is possible for these faults. The hazard potentials usually are so low for disturbances in the other category that continued network operation with a sustained fault is possible. The fault resistances reached their minimum values in the very beginning of the disturbances. However, some faults evolve gradually, for example faults caused by a broken pin insulator, snow burden, downed conductor, or tree contact. These faults are possible to detect from the change of neutral voltage before the electric breakdown. Transients could be detected in nearly all fault occurrences that demanded the function of the circuit breaker. In addition, about 70% of the transients were oscillatory. Characteristics of these phenomena can be made use of in the relay protection systems and in fault distance estimation.

4. Methods for high impedance earth fault indication and location

High impedance faults are difficult to detect with conventional overcurrent or neutral voltage protection devices because the zero sequence voltage or the fault current may not be large enough to activate them. In the past two decades many techniques have been proposed to improve the detection and location of these faults in distribution systems (Aucoin & Jones 1996). A short review of the existing methods is presented in Section 4.1. In Section 4.2, a new method is presented for the detection and location of high resistance permanent single-phase earth faults. We have developed the method further in Sections 4.3 and 4.4, and two alternative probabilistic approaches are proposed for the faulty feeder and line section location.

4.1 Review of the indication and location methods

The conventional method for permanent, high impedance fault detection is to use zero sequence overvoltage relays or to monitor the slight and fast variations in the neutral voltage. The faulted feeder can be found by transferring the supply of one feeder at a time to another substation and by observing the biggest change in the neutral voltage (Lamberty & Schallus 1981). However, this is time consuming. The other indication and location methods proposed in the literature, are based on the direct measurement of the basic components of the currents and voltages, on analysing their variations or their harmonic components with different methods, or on mixed versions of these methods.

4.1.1 Direct measurements of the electric quantities

The ratio ground relay concept, as implemented in the prototype relay, relies on tripping when the ratio of $3I_0$, the zero sequence current, to I_1, the positive sequence current, exceeds a certain pre-set level. This concept is implemented using an induction disc type relay with two windings. The operating winding produces torque proportional to $(3I_0)^2$ and the restraint winding produces torque proportional to $(I_1)^2 - (I_2)^2$. The two opposing torques produce the ratio trip

characteristic desired (Lee & Bishop 1983). The sensitivity of the method in an earth fault test was only 700 Ω. ABB (1997, 1995) has equipped some relays and fault indicators with a definite time current imbalance unit. Monitoring the highest and the lowest phase current values detects the imbalance of the power system i.e. the imbalance = $100\%(I_{L\max} - I_{L\min})/I_{L\max}$. Primarily, the algorithm is intended to indicate a conductor break, which can lead to a high impedance fault in the overhead network.

Roman & Druml (1999) have developed a so-called admittance method for the compensated networks, which measures the zero sequence currents of all feeders of the bus centrally. In addition, the phase and zero sequence voltages are required as a reference. Out of these values, the zero sequence admittances for each feeder are calculated and continuously monitored. The feeder with the highest alteration of the zero sequence admittance is identified as the faulty feeder. It is also possible to locate the fault point by connecting the faulted line and one sound line to a loop. The measured zero sequence current differences in the beginning of the looped lines are proportional to the ratio of the zero sequence admittance up to the fault location. The system detected faults of 30 kΩ in real field tests. Nikander & Järventausta (1998) and Nikander et al. (2000) have used the same principles for compensated and unearthed networks. Every feeder terminal operates independently, with no need to transfer information between the feeder terminals or between feeder terminals and upper level automation systems before indication of an event. Faults of 186 kΩ were reported to be detected and located in the preliminary field tests.

High resistance permanent earth faults in compensated systems can be detected by observing the neutral to ground voltage (Winter 1988). Three parameters, the mismatch, the damping (Brandes & Haubrich 1983) and the imbalance (Poll 1981, 1983) illustrate the symmetrical conditions of the network. The characteristic of the relative neutral voltage as a function of the mismatch is a tangent circle of the neutral point. It can be determined by measuring the change of the neutral voltage, when a small serial reactance is switched on to the suppression coil for a short time. The other parameters, the imbalance and the damping can be determined from the characteristic. The damping is the ratio of the resistive leakage current to the capacitive zero sequence current. The resistive earth fault changes the damping parameter. This can be detected by

continuously monitoring the neutral voltage characteristic. The sensitivity of the method was reported to be about 130 kΩ (Winter 1988).

Leitloff et al. (1997) developed three different algorithms to detect resistive faults and to select the faulty feeder in a compensated network. The static algorithm is based on a vector comparison of the residual currents in all the feeders. This comparison is carried out by taking a reference phase constructed from the sum of the residual currents of all the feeders, which is equal to the neutral current. The sensitivity was about 33 kΩ. The variant of the static algorithm is identical to the basic version but it is applied to the variations of the measured electrical quantities. The third algorithm enables fault detection by using the phase to ground admittance. As with the dynamic version, it makes use of the variations of the residual current. In addition to that, the variation of the neutral to ground voltage, the phase to ground voltages and the values of the global phase to ground admittances of the feeders before the fault occurrence are needed. It requires a periodic injection of a residual current by an automatic tuning system for the arc suppression coil (Chilard et al. 1999). The sensitivity of the last two mentioned algorithms was reported to be about 100 kΩ (Leitloff et al. 1994). The compensated systems pulse method, where the compensation degree is altered in a pulse-wise manner, can also be used for the identification of the faulty line (Christgau & Wolfenstetter 1982, Crucius & Kries 2001).

4.1.2 Harmonic analysis

High impedance ground faults generate harmonics because of a nonlinear resistance at the conductor-ground interface. Jeerings & Linders (1990) proposed that the change in the phasor value of the third harmonic current component is a sufficient criterion for fault indication in many cases. The harmonic change is measured by comparing a signal, which is averaged over a short period of time (1–2 seconds) with one averaged over a longer period (20–30 minutes) in one relay application (Atwell et al. 1990). A relay sensitivity of 1% of the current transformer rating has been achieved (Reason 1994). Yu & Khan (1994) used the magnitudes of the 3^{rd} and 5^{th} harmonic currents and the angle of the 3^{rd} harmonic current.

In frequency domain analysis, using Fourier transforms, many methods compare the odd harmonics or non-harmonics of the phase current. Russell et al. (1988) have used the 180 Hz and 210 Hz harmonic components. The fundamental frequency of the electric power system in this latter case was 60 Hz. Shiping & Russell (1991) proposed the energy algorithms, which monitor the energy variations of the phase current at a particular frequency or frequency band in the range, 2–10 kHz. The time is used as an element to discriminate high impedance faults from normal system events. A detector is also designed for monitoring the energy variance for the second, fourth and sixth harmonics of the residual current $3I_0$, and by requiring the increment of randomness of all these harmonics to indicate the fault (Lien et al. 1999). Randomness algorithms exploit the accompanying arc phenomena of intermittent arc re-ignition and extinction in the frequency band from 2 kHz to 3.6 kHz (Benner et al. 1989). Sultan et al. (1994) designed an arcing fault detector, which exploits the random behaviour of the fault current by comparing the positive and negative current peaks in one cycle to those in the next cycle, in order to measure the flicker and the asymmetry. Girgis et al. (1990) applied Kalman filtering theory to obtain the best estimation of the time variations of the fundamental and harmonic components, so as to avoid errors caused by conventional Fourier or classical filtering.

The algorithms mentioned above are not fully successful. This is either because of being unable to detect high impedance faults with very low current or is due to false tripping during normal system switching events, which produce similar transients to those of high impedance faults (Russell & Chinchali 1989). To mitigate these problems, Russell & Benner (1995) recommended a comprehensive expert system, which combines the above algorithms. A commercial device is also available (Benner & Russell 1997).

Recently, some new methods have been proposed for the purpose of better fault detection. Kim & Russell (1995) developed an algorithm to analyse the transient behaviour of various events on distribution feeders by quantifying wave distortion with the crest factor. Mamishev et al. (1996) and Huang & Hsieh (2001) have described some applications of the concepts of fractal geometry to analyse the chaotic properties of high impedance fault currents. The existence of chaotic behaviours are proved by evaluating fractal dimensions and the phase plane (Ko et al. 1998). Jota & Jota (1998) developed a fuzzy reasoning system

for the analysis of the feeder responses to impulse waves, which are periodically injected at the feeder inlet. These responses are compared to standard responses, which were previously stored in a database in the frequency range from 6 kHz to 12.5 MHz.

Because of fast response and efficient learning, Artificial Neural Networks have been applied in several electric power applications. Sultan et al. (1992) trained a neural network based detector using the Backpropagation algorithm, and Butler et al. (1997) used supervised clustering based neural networks. Wai & Yibin (1998) have used wavelet transform, which features variable time-frequency location rather than the windowed Fourier Transform. The transient signal can be decomposed in both the time and frequency domains via the wavelet transform, enabling more efficient monitoring of fault signals as time varies. The proposed methods have been applied to discriminate high impedance faults from normal switching events (Huang & Hsieh 1999). Vaughan & Moore (2000) have proposed a detection system based on very low frequency radio waves (VLF) from 3 kHz to 30 kHz. Shihab & Wong (2000) and Tungkanawanich et al. (2000) have proposed systems utilising the very high frequency radio waves (VHF), from 30 MHz to 300 MHz, released during arcing faults.

4.2 Neutral voltage and residual current analysis

A new method for high resistance fault detection and location, based on the change of neutral voltage and zero sequence currents, is presented in Paper C. The method consists of two independent algorithms, called neutral voltage analysis and residual current analysis.

The fault impedance $\underline{Z}_f$, of the neutral voltage analysis algorithm, can be determined in terms of the measured positive-sequence and zero-sequence voltages, and the zero-sequence impedance of the network as follows (Lehtonen 1998):

$$\underline{Z}_f = \left(\frac{\underline{U}_1}{\underline{U}_0} - 1 \right) \underline{Z}_0 \tag{18}$$

where $\underline{Z}_0$ is the zero-sequence impedance of the network**.** In an unearthed network, $\underline{Z}_0$ is the parallel connection of the phase-to-ground capacitances and phase-to-ground resistances, the so called ”leakage resistances”. For systems earthed via a Petersen coil, the circuit must be complemented with parallel connection of the coil impedance. For the detection of a high resistance earth fault, it is essential to determine the resistive part of the fault impedance. In eq. (18), $\underline{U}_0$ represents the phasor sum of the phase voltages and $\underline{U}_1$ is the positive sequence component of the phase voltage, measured at the moment considered. Applying eq. (18) for three times and using for $\underline{U}_1$ the following values: $\underline{U}_1$, $\underline{a}\underline{U}_1$ and $\underline{a}^2\underline{U}_1$, the faulted phase can also be determined. Here $\underline{a}$ is the phase shift operator, $\underline{a} = 1 \angle 120^o$.

From the three calculated values of $\underline{Z}_f$, the resistive part shows the highest value in the faulted phase. Because the fault impedance must be resistive, the calculated resistive parts of $\underline{Z}_f$ for the other two ”healthy” phases are negative. The triggering level of the algorithm is set so that a high resistance earth fault is indicated, if the calculated maximum real part of $\underline{Z}_f$ is smaller than the fixed threshold value and is at least four times the magnitude of the imaginary part of the corresponding $\underline{Z}_f$.

The detection of very high fault resistances is difficult due to the neutral voltage present in the normal network conditions. This is mainly caused by the natural imbalances of the feeders. The sensitivity of the method can be improved by using the change in the neutral voltage, which is determined as a difference between the real neutral voltage in the network at the moment being considered and the corresponding mean value of the last ten minutes. After calculation of the fault impedance $\underline{Z}_f$, and supposing that the fault resistance is very much higher than the network zero sequence impedance ($\underline{Z}_f >> \underline{Z}_0$), the earth fault current can be solved as follows

$$\underline{I}_f = \frac{\underline{U}_1}{\underline{Z}_f} \tag{19}$$

The faulted feeder is most often located by comparison of the residual current magnitudes. The residual current algorithm presented in Paper C utilises the simultaneous changes of neutral voltages and residual currents. The idea of the

algorithm is to compensate the effect of the earth capacitances by using the measured change of the neutral voltage and the known zero sequence impedance of the feeder under consideration (Lehtonen 1999).

$$\Delta \underline{I}_{0i} = \Delta \underline{I}_{0im} - \frac{\Delta \underline{U}_{0m}}{\underline{Z}_{0i}} \tag{20}$$

where $\Delta \underline{I}_{0i}$ is the compensated zero sequence current of the feeder i, $\Delta \underline{I}_{0im}$ is the measured change of zero-sequence current of the feeder i, $\Delta \underline{U}_{0m}$ is the measured change in the neutral voltage (zero sequence voltage) and $\underline{Z}_{0i}$ represents the zero-sequence impedance of the feeder i (including both the earth capacitance and leakage resistance).

Depending on the measurement accuracy, the resulting compensated current of a healthy feeder is nearly zero and in the case of the faulty feeder, it corresponds to one third of the earth fault current at the fault point. This method can also be used to discriminate the faulty line section, if the disconnector stations are provided with modern remote terminal units. This method requires accurate knowledge about the zero sequence impedances of each feeder. An advantage of the method is that, in the case of auto-reclosure, modern relays restore the values of the neutral voltage and zero sequence currents in the healthy feeders. These values can be used to update the zero sequence impedance data. When combining this information with the knowledge of the compensated zero sequence currents and the faulty phase, a very powerful means for detecting the faulty feeder, and further the faulty branch of the line, can be implemented.

4.3 Probabilistic approach

In the case of very high fault resistances, the magnitudes of the compensated feeder currents are small. Therefore, instead of direct comparison, it is more reasonable to quantify a probability estimate of whether the feeder concerned has failed. The compensated current values of the feeders and the estimated fault current are later regarded as random variables. These are assumed to be independent and identically distributed random variables obeying Normal distributions, with parameters μ = mean and σ^2 = variance (Taylor & Karlin

1984). In Paper D, two different probabilistic methods, the point probability method and the overall probability method, are presented.

In the point probability method, the expected fault current is modelled by a fixed value I_f. For the method, two different probability density functions are defined. Let $i = 1, \ldots, n$ denote feeders at the substation and variables $x_1, \ldots, x_n$ the possible compensated current values. Now, the current density function of a "healthy" feeder is denoted by $f_0(x)$. Since the compensated current values of the sound feeders should be zeros, the mean of $f_0(x)$ is also taken to be zero, i.e., $\mu_0 = 0$. The second probability density function is that of the faulty feeder, denoted by $f_1(x)$. In this case, the mean value should be equal to the expected fault current, $\mu_1 = I_f$.

Assuming that there is one fault in the network, the probability that feeder i has failed is, according to the Bayesian theorem (Box & Tiao 1973):

$$\Pr\left(\textit{feeder i has failed} \middle| I_{01},\ldots,I_{0n}\right) = \frac{\dfrac{f_1(I_{0i})}{f_0(I_{0i})}}{\displaystyle\sum_{i=1}^{n}\frac{f_1(I_{0i})}{f_0(I_{0i})}} \tag{21}$$

The point probabilities, in the cases of healthy and faulty feeders, are obtained by substituting the compensated current values I_{0i} to the normal distribution density functions $f_0(x)$ or $f_1(x)$, respectively.

In the second method, the expected fault current value I_f is no longer fixed but is assumed to be a random variable having a normal density function. Instead of the point probability value $f_1(x_i)$, the expected value $\overline{f_1(x_i)}$ is used.

$$\overline{f_1(x_i)} = \frac{1}{\sqrt{2\pi\left(\sigma_{1C}^2 + \sigma_{1U}^2\right)}} e^{-0.5\left(\frac{\mu_{1C}-\mu_{1U}}{\sigma_{1C}^2+\sigma_{iU}^2}\right)^2} \tag{22}$$

where μ_{1C}, σ_{1C}^2 and μ_{1U}, σ_{1U}^2 are the corresponding parameters of the normal distribution functions of the feeder current and expected fault current. In this

case, the mean values of the fault currents are supposed to be $\mu_{1U} = I_f$ and $\mu_{1C} = I_{0i}$.

When the maximum and minimum observed values of the compensated feeder currents, $I_{\max}$ and $I_{\min}$, are not taken into account, the sound feeder current variance is calculated as follows:

$$\sigma_0^2 = \frac{1}{n-2}\sum_{i=1}^{n}(x_i - \mu_0)^2 \tag{23}$$

The failed feeder current variance is derived in Paper D as:

$$\sigma_{1C}^2 \cong \left(\frac{I_{\max}}{3I_{ave}} + \frac{2}{3}\right)\sigma_0^2 \tag{24}$$

In the case of an unearthed network, the variance σ_{1U}^2 of the current density function $f_{1U}(x)$ can be defined as:

$$\sigma_{1U}^2 \cong (1+n)\sigma_0^2/3 \tag{25}$$

Depending on the compensation degree in resonant earthed networks, the variance of the current density function can be presented as follows:

$$\frac{(1+n)\sigma_0^2}{3} \le \sigma_{1U}^2 \le \frac{(1+200n)\sigma_0^2}{3} \tag{26}$$

The lower boundary is equal to the variance determined for the unearthed network.

4.4 Prototype system

The practical implementation of the method requires a close integration of the substation SCADA with modern relays, which are designed to be used for protection and control of the distribution network. A close connection to the

remote terminal units in the line locations is needed as well. PC based prototype version for the high impedance earth fault indication and location was developed for testing and simulation purposes, and it was coded with C-language. The system based on the network configuration, which is presented in Fig. 19, where the measurable variables are also presented. The relay functions were modelled as procedures. The procedures read the network parameters and the current and voltage samples from files as input data.

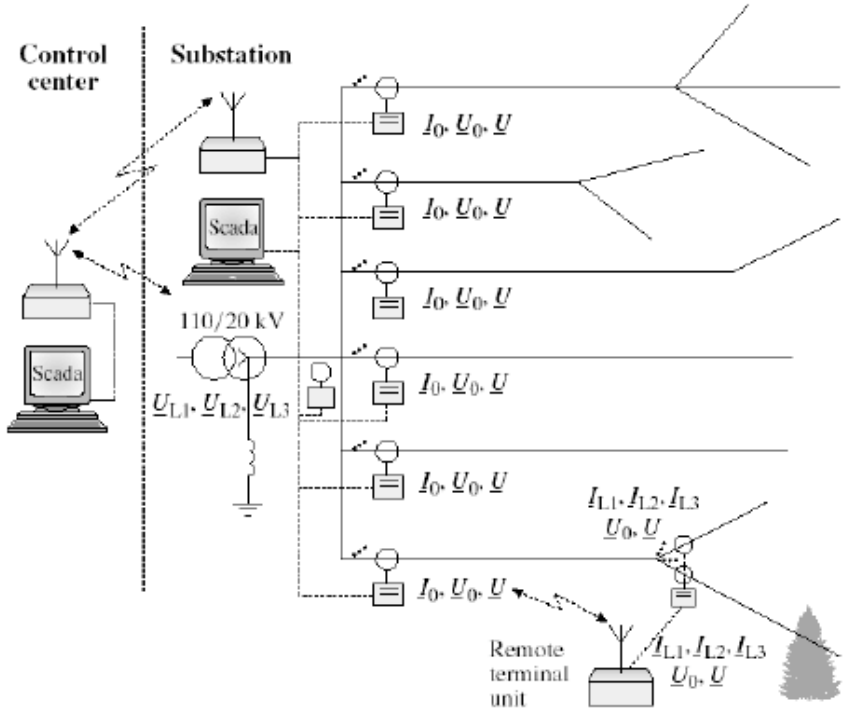

Figure 19. High resistance indication and location system.

The main functions of the prototype system consisted of the following procedures:

1. Measurement procedure in neutral voltage relay
2. Measurement procedure in feeder protection relays
3. Measurement procedure in disconnector substation

Program components in substation SCADA-computer

1) Procedure, which process the measurements and switching actions
2) Procedure, which updates the zero sequence impedances of the network and each feeder.

The computation uses the phasor form for currents, voltages and impedances. These parameters are computed as one second mean values and ten minutes sliding values. Without going to details, the high resistance indication and location system is intended to work briefly in the following way. The neutral voltage algorithm runs continuously in neutral voltage relay. It computes, among other things, the values of fault impedance, neutral voltage and its sliding mean value and the faulty phase. Also the residual current function runs continuously in each feeder protection relay and computes among other things the value of the sum current and the highest changes of the sum current and the neutral voltage during the last ten minutes. The same parameters are also computed in the disconnector terminal unit, if the feeder is equipped with remote controlled and readable disconnector. The time stamps of all measurements are also stored.

If the resistive part of the fault impedance is below the alarm or fault limit, the neutral voltage relay sends an event to the SCADA computer, which reads the value of fault impedance and the changes of neutral voltage and sum currents from each feeder and remote terminal unit. In this phase, the states of switches and connections are checked and stored. In the case of high resistive fault, the procedure of SCADA computer calculates the compensated sum current values for each feeder and if needed, for feeder branches. Using these current values, the faulty feeder or faulty branch is located based on the probabilistic method or on the magnitudes of the compensated sum currents.

In the case of auto-reclosure or permanent low resistance fault, the changes of neutral voltage and sum current of each sound feeder are stored during the fault. The SCADA procedure uses these values for updating the zero sequence impedances of the feeders and the whole network. These impedances must be also updated if the connection of network changes. Table 1 and Papers C and D show some computed results, when the earth fault test data from Kitee substation were used as an input data. The results showed that the method is able to detect and locate resistive earth faults up to a resistance of at least 220 kΩ. The first column of the Table 1 contains the exact values of the fault resistances (R_f) and

the phase to which the fault resistance was connected in the tests. The second column shows the complex phasors of the fault impedances ($\underline{Z}_f$), which were calculated from Eq. (18) using the voltage measurement values during the earth faults. The column titled ΔI_{0i} shows the compensated residual currents of the five feeders. These current values were determined by Eq. (20) and in the next column, I_f is the fault current obtained by Eq. (19).

Table 1. Detailed results for detection of the failed feeder with two alternative probabilistic method in the case of high resistance earth fault with the fault resistances 180–220 kΩ.

Phase, R_f [kΩ]	**$\underline{Z}_f$ [Ω]**	**ΔI_{0i} [A]**	**I_f [A]**	**$Pr(i\|x)_I$**	**$Pr(i\|x)_{II}$**	**Deviations**
L1 180	132970.45 - j*57056.70	0.0338 **0.1413** 0.0105 0.0350 0.0285	0.115	0.000524 0.998335 0.000179 0.000558 0.000403	0.000115 0.999673 0.000013 0.000128 0.000070	σ_o = 0.0325 σ_{om} = 0.0379 σ_{1C} = 0.0551 σ_{1U} = 0.0535 σ_{1Um} = 0.1778
L1 200	149451.84 - j*36034.95	0.0445 **0.1427** 0.0192 0.0601 0.0555	0.109	0.026388 0.881241 0.012957 0.042515 0.036899	0.006102 0.952745 0.000410 0.024173 0.016570	σ_o = 0.0538 σ_{om} = 0.0538 σ_{1C} = 0.0671 σ_{1U} = 0.0761 σ_{1Um} = 0.1545
L1 220	165731.73 - j*78135.77	0.0312 **0.1247** 0.0095 0.0307 0.0270	0.091	0.000749 0.997669 0.000254 0.000730 0.000597	0.000220 0.999419 0.000016 0.000209 0.000136	σ_o = 0.0297 σ_{om} = 0.0331 σ_{1C} = 0.0476 σ_{1U} = 0.0468 σ_{1Um} = 0.1556
L2 200	122712.48 - j*15709.50	0.0500 **0.2091** 0.0203 0.0592 0.0643	0.135	0.001931 0.991718 0.000886 0.002526 0.002939	0.001149 0.993298 0.000107 0.002248 0.003199	σ_o = 0.0581 σ_{om} = 0.0581 σ_{1C} = 0.0795 σ_{1U} = 0.0822 σ_{1Um} = 0.1778

These ones were calculated from the current and voltage values, which were measured in the beginning of the feeders at the Kitee substation. Faulty feeder is marked in bold. The column $Pr(i|x)_I$ shows the fault probability for each feeder determined by the point probability method. The corresponding probabilities $Pr(i|x)_{II}$, determined by the overall probability method, are in the following column. The last column shows the estimated deviations. The deviations σ_{0m} and σ_{1Um} are determined by iterating according to Paper D, if the initial values for the deviations were too small.

4.5 Discussion of the indication and location methods

A review of the existing techniques shows that many methods have been proposed for dealing with the high impedance fault detection problem. Several of these techniques have been implemented, either at the prototype level or at the production level; others have only been suggested. There are two distinct, competing parts to the high impedance fault problem: reliability and security. Reliability defines an algorithm's ability to detect faults sensitively, while security defines its ability to be immune from false detection when encountering a wide variety of other distribution system events. Security is at least as difficult to achieve as reliability.

Harmonic analysis cannot satisfactorily distinguish the disturbances of arcing faults from many switching events. A neural network approach, which trains the behaviour of the harmonic algorithm, still cannot successfully discriminate arcing faults and capacitor bank switching events. When encountering different disturbances, the neural network structure needs to be reorganised, plus the training process must be performed again. The reason for only partial success in discrimination is that when there is a disturbance, except in a few cases, the frequency domain information of the disturbance contains almost all the harmonic components. Thus it is not easy to find the one or two essential harmonic components that will discriminate one disturbance from another (Kim & Russell 1995). In Fourier transform based approaches where a window is used uniformly for spread frequencies, the wavelet uses short windows at high frequencies and long windows at low frequencies. In other words, by utilising wavelets, both time and frequency information can be obtained. However, the effectiveness of this method is highly dependent on the selection of a suitable

basis function. Poor selection of the basis function may inversely degrade the performance. The problems with radio waves are that the signals are greatly influenced by noise and interference from the surrounding area. In addition, the methods based on the harmonic analysis have been tested only in networks that are grounded via a small resistor.

According to experience gained from field tests in a 20 kV distribution system, the methods presented in Papers C and D are able to detect and locate resistive earth faults up to a resistance of at least 220 kΩ. The results clearly showed that in all cases, the highest fault probability was computed for the feeder where the earth fault really was. It would be possible to develop the method further to monitor the isolation state of a network continuously. From the practical point of view, the algorithms are also possible to implement to the modern numerical relays.

The problems of the algorithms, proposed in Papers C and D, are similar to those mentioned above. The drawback is that normal system activity and intermittent disturbances may cause changes to the neutral voltage and residual currents similar to the real faults in the feeders. Examples of these are normal switching actions, thunderstorms and snowfall. Thunderstorms and snowfalls can be discriminated by the fact, that they usually affect several feeders simultaneously. Using longer duration average measurements for comparison can mitigate the switching action problem, when identifying the faulty feeder or line section.

When applying the probabilistic methods, difficulties may arise if the sound feeder current distribution $f_0(x)$ is very narrow due to the small deviation. In these cases, the maximum feeder current value observed (I_{max}) does not fit the distribution, and the point probability is zero, $f_0(I_{\max}) = 0$. Problems may also occur if the deviation is too great. This is especially the case in the compensated network, where the variance σ_{1U}^2 may be too broad for the successful location of the failed feeder.

5. Low resistance earth fault distance estimation based on initial transients

One of the prime objectives when developing the automation of the distribution networks is the indication and location of earth faults. In this chapter, the fault distance estimation in radial operated networks is discussed based on charge transients. The existing solutions are first reviewed. Next, the signal pre-processing is described. The developed differential equation, wavelet and two different artificial neural network methods are then described. At the end of the chapter, the estimation accuracy of the methods is compared and the possible error sources are analysed.

5.1 Review of the fault distance estimation methods

Methods based on the calculation of the faulty line impedance, on the fault generated travelling waves, and on the Artificial Neural Networks are very promising, when the fault distance is estimated using current and voltage measurements derived from the substation in radial operated networks. In the travelling wave method, information about the fault position can be determined from the time difference between the incident travelling wave and its reflections. Bo et al. (1999) and Liang et al. (2000) have used transient voltage signals, and Xinzhou et al. (2000) have applied current travelling waves and wavelet transform. The main restrictions are the need of a very high sampling rate, in the range of MHz, and the difficulty to analyse the travelling waves and then extract the fault information if the feeder has several branches (Abur & Magnago 2000).

Ground fault initial charge transients can be utilised for line impedance estimation. Schegner (1989) presented a very promising differential equation algorithm. The second proposed technique employed Fourier-transform methods, which solve the line impedance in the frequency domain. The reactance of the faulty line length is obtained directly as the imaginary part of the impedance calculated from the corresponding frequency spectrum components of the voltage and current (Igel 1990, Igel et al. 1991). Lehtonen (1992) developed a least-squares fitting method, which uses a modification of Prony's method for estimation of the transient parameters. The average error in

field tests is reported to be a little more than 1 km when the fault resistance is 0 Ω, and the sampling rate is 10–20 kHz (Lehtonen 1995). Eickmeyer (1997) applied the neural network method trained by the transient samples of current and voltage signals. However, the accuracy of that method was tested only by simulated data.

In the following sections, four new algorithms are described. The aim of these methods is that they allow online calculations in numerical relays. The main advantage is the numerical stability and relatively small computation burden using the sampling rate of 5 kHz. The differential equation method is essentially an impedance relay algorithm and therefore, it is suitable for this purpose. The wavelet algorithm and the ANN algorithms also provide a fast response. In addition, a second ANN algorithm is proposed, which needs only one measurement per primary transformer.

5.2 Signal pre-processing

The fault distance estimation algorithms are intended to work in the feeder protection relays, in spite of the second ANN algorithm, so called ANN Uo-algorithm, which is intended to work in the zero sequence overvoltage relay. In the first mentioned case, some network periods of phase voltages and phase currents are needed to measure before and during the fault including the transient. In the case Uo-algorithm, some network periods of zero sequence voltage have to be measured. The measured voltage signal contains in addition to the fundamental both its harmonic components and the transient components. The current signal contains the following components (Lehtonen 1992):

– fundamental (50 Hz) component of the load current and its harmonics
– fundamental (50 Hz) component of the fault current and its harmonics
– charge transient component
– discharge transient component
– interline compensating transient component
– a decaying DC-transient of the suppression coil circuit.

The charge component has a lower frequency than the discharge component and it dominates the amplitudes of the composite transient. The signal pre-processing covers the extraction of the dominating transient component from the other signal parts in the following steps:

1) removal of the fundamental frequency component
2) spectrum analysis for estimating the charge transient frequency
3) low-pass filtering in order to remove the higher frequency components

For the fundamental frequency removal a straightforward technique is used: $g(t) = f(t) - f(t + T)$, where $g(t)$ is the output of the filter, $f(t)$ is the original signal and T is the period of the fundamental frequency. The spectrum analysis is performed by a Fourier algorithm, which covers only a 20 ms window, starting from the beginning of the transient. The frequency band used is from 100 Hz to 833 Hz, corresponding to a 5 kHz sampling frequency. The highest amplitude spectrum component is assumed to be the one corresponding to the charge transient frequency. The cut-off frequency of the low-pass Bessel filter is set 400 Hz higher than the estimated charge transient frequency (Schrüfer 1990). The measured signals are processed in a reversed order. Similar signal pre-processing is applied to all the algorithms considered.

5.3 Differential equation method

Differential equation algorithms solve the line inductance directly in the time domain, if three equally spaced pairs of phase current and voltage samples are available as follows (Phadke & Thorp 1990):

$$L = \frac{\Delta t}{2}\left[\frac{(i_{k+1}+i_k)(u_{k+2}+u_{k+1})-(i_{k+2}+i_{k+1})(u_{k+1}+u_k)}{(i_{k+1}+i_k)(i_{k+2}-i_{k+1})-(i_{k+2}+i_{k+1})(i_{k+1}-i_k)}\right] \tag{27}$$

The above equation yields the total inductance of the faulty line length, which in the case of a single phase to earth fault is composed of a series connection of zero-, positive- and negative-sequence inductances.

$$L = \frac{1}{3}\left(L_1^{'} + L_2^{'} + L_0^{'}\right) \cdot l \tag{28}$$

In this study, the differential equation algorithm is used in its basic form as described in Eq. 27, see Paper E. The computation is made first for a window of 12 subsequent samples. In this phase, Equation (27) is applied for 10 different three sample sets, and the average value and statistical deviation is computed for the inductance estimates. This procedure is repeated for 20 time, shifting the starting point gradually forward. The final estimate of the inductance is the one having the smallest deviation.

5.4 Wavelet method

The distance estimation is based on the computation of the wavelet coefficients for voltage and current transients, see Paper E. The discrete wavelet transform was used to find the complex wavelet coefficients W_s. Let us call Δt the sampling period, k and n are integers, and f_c is the estimated charge transient frequency. For a chosen frequency f and for a "location" of wavelet $k\Delta t$:

$$W_s(k\Delta t, f) = \sum_n s(n\Delta t) \cdot \sqrt{f / f_c} \cdot \overline{\Psi}\left[(f / f_c) \cdot (n\Delta t - k\Delta t)\right] \cdot \Delta t \tag{29}$$

After examination of several kinds of wavelet (Chui 1992, Rioul & Vetterli 1991, Weiss 1994), the following complex "mother wavelet" $\Psi(t)$ was chosen (Chaari et al. 1996):

$$\Psi(t) = \left(1 + \sigma|t| + \frac{\sigma^2}{2}t^2\right) e^{-\sigma|t|} e^{i\omega \cdot t} \tag{30}$$

The earth fault distance can be estimated by first calculating the inductance as follows:

$$L = \frac{1}{\omega}\mathrm{Im}\left[\frac{U_w(k\Delta t, f)}{I_w(k\Delta t, f)}\right] = \frac{1}{3}\left(L_1^{'} + L_2^{'} + L_0^{'}\right) \cdot l \tag{31}$$

The algorithm first determines the maximum wavelet coefficient of the current including the amplitude, frequency and location of the wavelet. Using this frequency with different time translations, the equivalent fault inductances are calculated with equation (31). The 2 ms inductance interval, corresponding to 10 subestimates, is then determined with the smallest standard deviation. The mean value of the inductance, which is calculated in this interval, is finally used to determine the fault distance.

The differential equation and wavelet algorithms were about one and a half years in trial use on one feeder on two substations. There occurred altogether 8 permanent earth faults for which the fault distance could be computed. The results are in Table 2. In this case the sampling frequency was only 3.7 kHz, due to the limitations of the recorders.

Table 2. Calculated fault distances in the case of real earth faults, MEK= mean absolute error in kilometers.

			Diff. equation algorithm	Wavelet algorithm
Network grounding	Exact fault distance	Fault resistance	Error	Error
	[km]	[Ω]	[km]	[km]
Compensated network	9.5	19.8	–2.4	–1.9
Compensated network	22.2	30.2	–0.1	+0.8
Compensated network	18.5	96.2	–5.2	+7.5
Unearthed network	5.8	36.7	–0.3	–4.3
Unearthed network	13.6	104.8	+3.1	–0.1
Unearthed network	4.9	27.4	–0.2	+5.6
Unearthed network	13.8	27.7	+2.7	+0.6
Unearthed network	1.1	10.9	+3.2	–0.1
			MEK = 2.2	MEK = 2.6

5.5 Artificial neural network methods

The application of Artificial Neural Network (ANN) computing to power systems has a relatively short time span of about 10 years. The applications for

protective relays are still at an exploratory stage concerning fault distance estimation in distribution networks. So far applications have been developed for fault detection and classifications (Dalstein & Kulicke 1995), distance and direction detection (Sidhu et al. 1995), autoreclosure (Yu & Song 1998) and fault location (Bo et al. 2000) in transmission systems. The survey of ANN applications to protective relaying (Kezunovic 1997, Dillon & Niebur 1996) shows that almost all the applications use the multilayer perseptron type of the architecture with the basic three layers being a typical choice. The supervised learning with the Backpropagation learning rule was selected most often with few exceptions.

When applying ANN methods for fault distance estimation a result that can be predicted is desirable. The output of the ANN is a linear knowledge of the fault distance when real measured signals are used as input values. This means that the estimating fault distance is in the range of 0 km to the length of the longest feeder presented in kilometres. Due to these facts, the supervised learning of the ANN is the most suitable for this purpose. In the case of supervised learning for real signals, the most effective learning algorithm is the Backpropagation algorithm (Eickmeyer 1997), which is also used in this study. The optimal structure of ANN, concerning the number of hidden layers, the number of neurons in a layer and the size of the input and out put vectors, can only be determined empirically.

In Papers F and G, two transient based ANN algorithms are discussed. The ANN-structure called Multilayer Perceptron is used. It consists of the input vector, one hidden layer and the output layer. Haykin (1994) has proved that in general one hidden layer is sufficient for representing any given input-output transformation. Using more than one hidden layer is necessary if the pattern recognition task seems to be quite sophisticated and if there is a large number of input neurons. The number of hidden neurons n_j was varied in the range [$10 \leq n_j \leq 30$] for different neural networks. An example for choosing the optimal number of hidden neurons empirically is presented in Fig. 20.

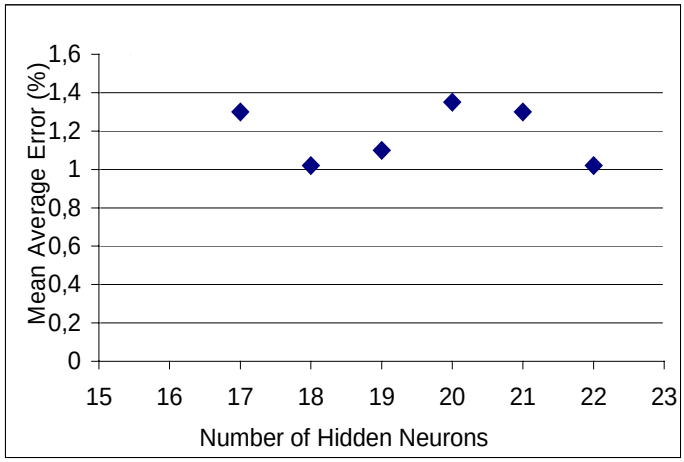

Figure 20. Mean average error in distance estimation for different numbers of hidden neurons for the network size of 300 km.

The algorithm in Paper F uses either the phase voltage or the phase voltage and current samples as input data. The second algorithm in Paper G uses the harmonic components of the neutral voltage transients as input data. As an output value, the fault distance is given by the activation of one single output neuron. The Backpropagation training algorithm provides a fast and stable training and a sufficient error decrease for the ANN. For implementation, training and verification of the ANN, the software MATLAB and its ANN toolbox were applied.

For training and testing of the ANN a large data set of voltage and current samples is necessary. The affecting parameters are varied within an appropriate range to provide the ANN with all the important features.

– fault distance: 1–40 km
– network size: 100–600 km
– load: 0–100 A
– load angle, cosΦ: 0.8–1
– network grounding: unearthed, compensated
– entrance angle: 0–90°
– fault resistance: 0.1–15Ω
– Phase: *L*1, *L*2.

Earth faults were simulated by the common simulation tool "Alternative Transients Program" (ATP-EMTP). The basic 20 kV overhead lines were modelled using the Line Constants ATP-EMTP Program and taking into account the real geometrical and electrical values.

A fault distance estimation system must be able to work properly in networks of different sizes, and under different load conditions and fault entrance angles; i.e. the phase to ground voltage angle that exists when the fault occurs. Paper F shows that, although good general performance is achievable, there was a small span in frequency and entrance angles where the ANN produced very exact results. The network size affects both the charge frequency and the amplitude of the transients. To decrease the huge training process different scaling methods were developed for the cases where input data adaptation is needed. In Paper F, the ANNs are trained either by phase voltage or phase voltage and current samples of transients, the network sizes being 150 km and 300 km for compensated and unearthed networks. The purpose of the time scaling is to move the actual frequency into the trained frequency band. Stretching or shortening the cycle period accomplishes the scaling of the frequency. For this kind of curve fitting a Pascal program that utilises the Newton method was developed. The transient current amplitude increases with enlargement of the power distribution network, but the amplitude of the transient voltage remains almost constant. The amplitude scaling factors for voltage and for current were determined by testing a number of simulated and measured data.

In Paper G, two different ANNs were trained for the network sizes of 300 km and 420 km, respectively. The purpose of the frequency scaling is to move the actual frequency into the trained frequency band. The network size and fault distance can be taken into account by utilising a linear function. The scaling factor (SF) for the spectrum of the harmonic components can be obtained as follows:

$$SF = \frac{f_0 - f_{30}}{f'_0 - f'_{30}} \tag{32}$$

The harmonic frequencies are multiplied by the scaling factor SF, meaning that the spectrum is stretched or shrunk while the amplitudes remain unchanged. The

scaled harmonic spectrum for the distance computation is finally determined by interpolation due to the fact that the harmonic frequencies must be the same as used for the ANN training.

5.6 Discussion of the distance estimation methods

It is possible to calculate an estimate for the position of single phase to earth faults. If the faulty feeder has several branches, there are also several possible fault locations. In this case, remotely read fault current indicators can complement the fault location system. In high impedance earthed networks, the charge frequency of the transient varies approximately in the range 100 to 800 Hz, and the amplitude can be as much as 15 times that of an uncompensated steady state fault current. This component is suitable for fault location purposes (Lehtonen 1992).

Four different algorithms were developed. The differential equation algorithm, the wavelet algorithm and the ANN algorithm trained by current and voltage samples require simultaneous measurements of the phase currents and voltages in the faulty feeder. The ANN algorithm, which uses the harmonic components of the neutral voltage transients, needs only one measurement per primary transformer. The developed methods were tested with the same field test data. In addition, the differential equation and wavelet algorithms were one and a half years in trial use in real network circumstances, see Table 2. Comparison of the conventional algorithms shows that both algorithms worked equally if all staged field tests are taken into account. In the case of real earth faults, the differential equation algorithms gave slightly more accurate results. Considering different earthing systems, the differential equation algorithm is more accurate in the partially compensated and unearthed networks, whereas the wavelet algorithm is better in the compensated case. The likely reason is, that transients are more oscillatory and the form of the wavelet used is more similar to the real transient in the compensated systems than in the other ones. On the other hand, the presence of the decaying DC component in the compensated network may have more influence on the calculation accuracy of the differential equation algorithm than on the accuracy of the wavelet algorithm.

The performance of the ANN methods was comparable to that of the conventional algorithms. Regarding only the earth faults with very low fault resistance, the ANN methods gave even better results, see Table 3. The mean error in absolute terms was about 1.0 km for ANN methods and about 2.0 km for the conventional algorithms in the staged field tests. The ANN with single voltage input samples reached an absolute mean error of 3.7 km. The conventional algorithms worked better with higher fault resistances. The ANN methods are also sensitive to the scaling in cases where input data adaptation is needed due to different network sizes. The usable results were achieved when the input data adaptation was small, i.e. when the scaling factor was in the range of 0.85 to 1.15.

Table 3. Comparison of different ANN methods using field test data. The errors are absolute mean values computed from the repeated earth fault tests.

Network earthing	Exact fault distance (km)	Fault resistance (Ω)	ANN methods		
			Voltage	Voltage/ current	U_0-spectrum
			error (km)	error (km)	error (km)
Compensated	0.76	0	2.4	0.7	1.7
Compensated	10.4	0	13.8	0.7	0.9
Compensated	14.2	0	2.7	1.3	0.2
Partially compensated	25.4	0	1.3	1.3	0.2
Partially compensated	36.0	0	0.9	1.0	2.5
Unearthed	13.3	47	7.9	5.9	5.0
Unearthed	20.0	47	13.8	15.2	5.8

The most important causes of errors in transient based fault distance estimation are parameter identification inaccuracy, measurement transformer errors, line model simplifications, line inductance variation and load impedances. If damping of the transient is small, the total error due to parameter identification is typically less than 2%. Fault resistance and resistive loads increase the attenuation, with a corresponding increase in the errors. In the tests, the highest fault resistance that allowed for reliable distance estimation was 50 Ω. Standard

current transformers have a good fidelity in the frequency range of transients. Unfortunately this is not always the case for voltage transformers. The errors of the line model simplifications primarily include the effect of ignored capacitances at the fault location and behind it. The maximum error due to these is, in typical overhead line networks, about 2%. One of the two major error sources is the variation of line inductances. The zero sequence inductances of an overhead line vary with the soil type and frequency. Perhaps the largest errors are, however, due to low voltage loads. Usually, neither the load devices nor their impedances during the transients are known well enough. The loads can cause large errors, especially in the case of distant faults and for fault resistances higher than zero.

The practical implementation of the algorithms requires the measurement of the neutral voltage in the case of the ANN U_0-spectrum algorithm, and the measurements of the phase currents and voltages of the feeder in the case of the other algorithms. ANN algorithms are sensitive to the changes of the network size for example due to the changes in connections of the network. Small changes are possible to manage with input data adaptation, but for bigger changes several ANNs are needed to train. For the time being, the practical implementation to the numerical relays is restricted by the sampling rate of the relays. The sampling rate of the numerical protection relays is 2 kHz nowadays. It should be 5 kHz for transient based methods at least.

6. Summary

The contribution of this thesis is to determine the characteristics of real earth faults in Finnish distribution network circumstances. Based on these characteristics new methods of earth fault indication and location were developed. Implementing these methods as new functions in distribution automation can decrease outage times.

In unearthed networks, more than a half of the disturbances were arcing faults. These can lead to overvoltages higher than double the normal phase to ground voltage. Only a few arcing faults occurred in compensated networks. Especially in the unearthed systems, the maximum currents that allowed for autoextinction were, in spite of the use of surge arresters, clearly smaller than had previously been believed. Fault resistances fell into two major categories, one where the fault resistances were below a few hundred ohms and the other where they were in the order of thousands of ohms. In the first category, faults are most often flash-overs to the grounded parts of the network. Distance computation is possible for these faults. In the second category, the majority of the faults disappeared of their own accord. However, a part of these faults evolve to the lower range of fault resistance, whereupon early detection is important.

Faults evolving gradually are, for example, caused by a broken pin insulator, snow burden, downed conductor or tree contact. Using the neutral voltage and residual current analysis with the probabilistic method, it is possible to detect and locate resistive earth faults up to a resistance of 220 kΩ. Practical implementation of the method requires a close integration of the substation SCADA with modern numerical relays. The location means the determination of the faulty feeder or line section. The field test results showed that in all cases, clearly the highest fault probability was computed for the feeder where the earth fault really was. The neutral voltage and residual current algorithms, developed during this study for high resistive fault indication and location, are possible to implement to the numerical relays.

This work also contributed to the development of new applications of the transient based differential equation, wavelet and neural network methods for fault distance estimation. The performance of the ANN methods was comparable to that of the conventional algorithms. It was also shown that the ANN trained

only by harmonic components of the neutral voltage transients is applicable for earth fault distance computation. The benefit of this method is that only one measurement per primary transformer is needed. Regarding only the earth faults with very low fault resistance (0 Ω), the ANN methods gave even better results than the other methods. The mean error in absolute terms was about 1.0 km for the ANN methods and about 2.0 km for the conventional algorithms in the staged field tests. The differential equation and wavelet algorithms were also in pilot use with a 3.7 kHz sampling rate in real network circumstances, where the differential equation algorithms gave slightly more accurate results. The restriction for transient based methods was that the highest fault resistance allowing reliable distance estimation was about 50 Ω. The drawbacks of the ANN methods were that they gave the best results when trained specifically for the one network size for which they were primarily intended. Small variations are possible to manage with input data adaptation, but for bigger changes of the network, several ANNs are needed to train. Therefore, from the techniques tested in this thesis, the differential equation algorithm seems to be the most promising alternative for transient based fault distance estimation. For the time being, the practical implementation of the transient based methods to numerical relays is restricted by the sampling rate of 5 kHz, which is needed.

This thesis has indicated several subjects worthy of further study:

- To avoid unnecessary auto-reclosings, the methods should be developed to discriminate arcing faults from permanent ones.

- The probabilistic method concerning the indication and location of high resistance faults should be developed further to monitor the isolation state of the network continuously.

- The signal pre-processing methods for fault distance estimation should be developed so that the transient effects of the filter itself do not affect the measured signals.

- The applicability of the differential and wavelet methods to fault distance estimation using only the measurements of the primary transformer supply bay should be analysed.

References

ABB. 1995. Fault indicator SPEF 3A2 C. Vaasa: ABB Network Control & Protection. 26 p.

ABB. 1997. SPAA 341 C Feeder Protection Relay. User's manual and technical description. Vaasa: ABB Network Partner. 149 p.

Abur, A. & Magnago, F.H. 2000. Use of time delays between modal components in wavelet based fault location. Electrical Power & Energy Systems. Elsevier Science Ltd. Pp. 397–403. (Vol. 22.)

Atwell, E.A., Shaffer, A.W., Jerrings, D.I. & Linders, J.R. 1990. Performance testing of the Nordon high impedance ground fault detector on a distribution feeder. 1990, Rural electric power conference. Paper presented at the 34th annual conference. NY, USA: IEEE. Pp. C6/1–7. (Cat. No.90CH2823-3.)

Aucoin, B.M. & Jones, R.H. 1996. High impedance fault detection implementation issues. IEEE Transaction on Power Delivery. IEEE. Pp. 139–144. (Vol. 11. No. 1, January.)

Benner, C., Carswell, P. & Russell, B.D. 1989. Improved algorithm for detection arcing faults using random fault behavior. EPSR (Electric Power Systems Research), Switzerland. Pp. 49–56. (Vol. 17, No. 1, July.) ISBN 0378-7796

Benner, C.L. & Russell, B.D. 1997. Practical high-impedance fault detection on distribution feeders. IEEE Transactions on Industry Applications. USA: IEEE. Pp. 635–640. (Vol. 33, No. 3, May/June.) ISBN 0093-9994

Blackburn, J.L. 1993. Symmetrical Components for Power Systems Engineering. New York, USA: Marcel Dekker, Inc. 427 p. ISBN 0-8247-8767-6

Bo, Z.Q., Weller, G. & Redfern, M.A. 1999. Accurate fault location technique for distribution system using fault-generated high-frequency transient voltage signals. IEE Proceedings – Generation, Transmission and Distribution. IEE. Pp. 73–79. (Vol. 146, January.)

Bo, Z.Q., Jiang, F., Chen, Z., Dong, X.Z., Weller, G. & Redfern, M.A. 2000. Transient based protection for power transmission systems. Proceedings of 2000 IEEE Power Society Winter Meeting. 23–27 January 2000. Singapore: IEEE. 6 p. (CD-ROM, 00CH37077C.) ISBN 0-7803-5938-0

Box, G.E.P. & Tiao, G.C. 1973. Bayesian Inference in Statistical Analysis. Addison-Wesley, Reading, MA. 588 p. ISBN 0-201-00622-7

Brandes, W. & Haubrich, H.J. 1983. Sterbpunktverlagerung durch mehrfach-leitungen in erdschlußkompensierten 110-kV-Netzen. Betriebliche erfahrungen und Abhilfemaßnahmen. Elektrizitätswirtschaft. Frankfurt: VDEW. Pp. 400–405. (Jg. 82, Heft 11.) ISBN 0013-5496

Butler, K.L., Momoh, J.A. & Sobajic, D.J. 1997. Field studies using a neural-net-based approach for fault diagnosis in distribution networks. IEE Proceedings – Generation, Transmission and Distribution. IEE. Pp. 429–436. (Vol. 144, No. 5, September.)

Chaari, O., Meunier, M. & Brouaye, F. 1996. Wavelts: A new tool for the resonant grounded power distribution systems relaying. IEEE Transactions on Power Delivery. USA: IEEE. Pp. 1301–1308. (Vol. 11, No. 3, July.) ISBN 0885-8977-96

Chilard, O., Morel, L. & Renon, D. 1999. Compensated grounded medium voltage network protection against resistive phase to ground faults. Proceedings of CIRED'99, 15th International Conference and Exhibition on Electricity Distribution, 1–4 June 1999, Nice, IEE, 4 p. (CD-ROM)

Christgau, G. & Wolfenstetter, W. 1982. Zuverlässige Ortungs und Melde-methode bei Erdschlüssen im Mittelspannungsnetz. In: Elektrizitätswitrschaft. Frankfurt: VDEW. Pp. 804–810. (Jg. 82, Heft 23.) ISBN 0013-5496

Chui, C.K. 1992. An introduction to wavelets. San Diego, USA: Academic Press, Inc. 264 p.

Claudelin, P. 1991. Compensation of the earth fault current in a MV distribution network. Earth fault problems in MV Systems. Helsinki: INSKO. Pp. 1–38. (INSKO 157-91.) (In Finnish)

Crucius, M. & Kries, G. 2001. Fehlersensoren – ereignisorientierte Wartung in Mittelspannungsnetzen. ETZ Electrotechnik + Automation. Berlin: VDE Verlag. Pp. 22–25. (Heft 3–4)

Dalstein, T. & Kulicke, B. 1995. Neural network approach to fault classification for high speed protective relaying. IEEE Transactions on Power Delivery. IEEE. Pp. 1002–1011. (Vol. 10, No. 2, April.) ISBN 0885-8977-95

Dillon, T.S. & Niebur, D. 1996. Neural networks applications in power systems. London: CRL Publishing Ltd. 404 p. ISBN 0-9527874-0-7

Eickmeyer, D. 1997. Einsatz kunstlicher neuronaler Netze bei der Ortung von Erdschlussen. Dissertation TU Berlin: 136 p.

Girgis, A.A., Chang, W. & Makram, E.B. 1990. Analysis of high-impedance fault generated signals using a Kalman filtering approach. IEEE Transactions on Power Delivery. USA: IEEE. Pp. 1714–1722. (Vol. 5, No. 4, November.)

Haase, H. & Taimisto, S. 1983. New Finnish Equipment for compensation of earth fault current. Sähkö, Electricity and Electronics. Pp. 48–51. (Vol. 56, 12. December.) (In Finnish)

Haykin, S. 1994. Neural networks – A comprehensive foundation. New York: MacMillan, Prentice Hall International Editions. 696 p.

Huang, S.J. & Hsieh, C.T. 1999. High-impedance fault detection utilizing a Morlet wavelet transform approach. IEEE Transactions on Power Delivery. USA: IEEE. Pp. 1401–1410. (Vol. 14, No. 4, October.) ISBN 0885-8977-99

Huang, S.J. & Hsieh, C.T. 2001. Feasibility of fractal-based methods for visualization of power system disturbances. Electrical Power & Energy Systems. Elsevier Science Ltd. Pp. 31–36. (Vol. 23.)

Hubensteiner, H. 1989. Schutztechnik in elektrischen Netzen. Offenbach/Berlin: VDE-Verlag. 282 p.

Igel, M. 1990. Neuartige Verfahren für den Erdschlußdistanzschutz in isoliert and kompensiert betriebenen Netzen – Signale und Algorithmen im Frequenzbereich. Dissertation. Universität des Saarlandes, Saarbrücken, Germany. 181 p.

Igel, M., Koglin, H.-J. & Schegner, P. 1991. New algorithms for earth fault distance protection in insulated and compensated networks. ETEP (European Transaction in Electrical Power). VDE Verlag. Pp. 253–259. (Vol. 1, No. 5, September/October.)

Jeerings, D.I. & Linders, J.R. 1990. Unique aspects of distribution system harmonics due to high impedance ground faults. IEEE Transactions on Power Delivery. USA. Pp. 1086–1094. (Vol. 5. No. 2, April.) ISBN 0885-8977

Jota, F.G. & Jota, P.R.S. 1998. High-impedance fault identification using a fuzzy reasining system. IEE Proceedings – Genration, Transmission and Distribution. IEE. Pp. 656–662. (Vol. 145, No. 6, November.)

Kezunovic, M. 1997. A survey of neural net applications to protective relaying and fault analysis. Engineering Intelligent Systems. CRL Publishing Ltd. Pp. 185–192. (Vol. 5, No. 4, December.)

Kim, C.J., Russell, B.D. 1995. Analysis of distribution disturbances and arcing faults using the crest factor. EPSR (Electric Power Systems Research), Pp. 141-148. (Vol. 35, No. 2.) ISBN 0378-7796

Klockhaus, H., Poll, J. & Sauerbach, F.J. 1981. Sternpunktverlagerung und Erdschlußfehlerortsuche im Mittelspannungsnetz. Elektrizitätswirtschaft. Frankfurt: VDEW. Pp. 797–803. (Jg. 80, Heft 22.) ISSN 0013-5496

Ko, J.H., Shim, J.C., Ryu, C.W., Park, C.G. & Yim, W.Y. 1998. Detection of high impedance faults using neural nets and chaotic degree. Proceedings of EMPD '98. 1998 International Conference on Energy Management and Power Delivery. 3–5 March. Singapore: IEEE. Pp. 399–404. (IEEE Catalogue No. 98EX137.) ISBN 0-7803-4495-2

Lakervi, E. & Holmes, E.J. 1995. Electricity distribution network design. 2nd Edition. England: Peter Peregrinus Ltd. 325 p. (IEE Power Engineering series 21.) ISBN 0 86341 309 9

Lamberty, G. & Schallus, K. 1981. Betriebserfahrungen mit der Ortung von Erdschlussfehlern vei unterschiedlicher Sternpunktbehandlung im 10-kV-Mittelspannungsnetz. Elektrizitätswirtschaft. VDEW. Pp. 803–809. (Jg. 80, Heft 22.) ISSN 0013-5496

Lee, R.E. & Bishop, M.T. 1983. Performance testing of the ratio ground relay on a four-wire distribution feeder. IEEE Transactions on Power Apparatus and Systems. IEEE. Pp. 2943–2949. (Vol. PAS-102, No. 9.)

Lehtonen, M. 1992. Transient analysis for ground fault distance estimation in electrical distribution networks. Espoo: The Technical Research Centre of Finland. 181 p. (VTT Publications 115.) ISBN 951-38-4233-9

Lehtonen, M. 1995. Method for distance estimation of single-phase-to-ground faults in electrical distribution networks with an isolated or compensated neutral. ETEP (European Transaction in Electrical Power). VDE-Verlag. Pp. 193–198. (Vol. 5, No. 3, May/June.)

Lehtonen, M. 1998. A Method for detection and location of high resistance earth fault in electrical distribution networks. Pat. FI. No. 100922, ABB Transmit Oy, publ. 13.03.1998.

Lehtonen, M. 1999. A Method for detection and location of high resistance earth fault in electrical distribution networks based on current measurements. Pat. FI. No. 103217, ABB Transmit Oy, publ. 14.05.1999.

Lehtonen, M. & Hakola, T. 1996. Neutral earthing and power system protection. Earthing solutions and protective relaying in medium voltage distribution networks. Vaasa: ABB Transmit Oy. 118 p. ISBN 952-90-7913-3

Leitloff, V., Pierrat, L. & Feuillet, R. 1994. Study of the neutral-to-ground voltage in a compensated power systems. ETEP (European Transaction in Electrical Power). Pp. 145–153. (Vol. 4, No. 2, March/April.)

Leitloff, V., Pierrat, L. & Feuillet, R. 1997. Detection of resistive single-phase earth faults in a compensated power-distribution system. ETEP (European Transaction in Electrical Power). Pp. 65–73. (Vol. 7, No. 1, January/February.)

Liang, J., Elangovan, S. & Devotta, J.B.X. 2000. Application of wavelet transform in travelling wave protection. Electrical Power & Energy Systems. Elsevier Science Ltd. Pp. 537–542. (Vol. 22. No. 8.)

Lien, K.Y., Chen, S.L., Liao, C.J., Guo, T.Y., Lin, T.M. & Shen, J.S. 1999. Energy variance criterion and threshold tuning scheme for high impedance fault detection. IEEE Transactions on Power Delivery. IEEE. Pp. 810–817. (Vol. 14, No. 3, July.)

Mamishev, A.V., Russell, B.D. & Benner, C.L. 1996. Analysis of high impedance faults using fractal techniques. IEEE Transactions on Power Systems. USA: IEEE. Pp. 435–440. (Vol. 11, No. 1, February.) ISBN 0885-8950

Mörsky, J. 1992. Relay protection techniques. Second edition. Hämeenlinna: Otatieto Oy. 459 p. ISBN 951-672-175-3 (In Finnish)

Nikander, A. & Järventausta, P. 1998. Methods for earth fault identification and distance estimation in a compensated medium voltage distribution network. Proceedings of international conference on Energy Management and Power Delivery '98 (EMPD '98). Singapore: IEEE. Pp. 595–600. (IEEE Catalogue No. 98EX137.) ISBN 0-7803-4495-2

Nikander, A. & Lakervi, E. 1997. A philosophy and algorithms for extinguishing earth fault arcs in suppressed medium voltage networks. Proceedings of CIRED'97, 14th International Conference and Exhibition on Electricity Distribution, 2–5 June 1997. IEE. Pp. 4.20.1–4.20.6. (Conference Publication No. 438.)

Nikander, A., Järventausta, P. & Rissanen, P. 2000. Methods for identification and distance estimation of high impedance earth faults in medium voltage networks. In: Lehtonen, M. TESLA – Information technology and electric power systems. Technology Programme 1998–2002. Interim report 1999. VTT. 8 p. (Tesla NR 27/2000.)

Paulasaari, H., Järventausta, P., Verho, P., Kärenlampi, M., Partanen, J., Hakola, T. & Vähätalo, E. 1995. Methods to study earth fault phenomena by using a residual overvoltage relay module. Proceedings of IEEE/KTH Stockholm Power Tech. Conference, Stockholm, Sweden, June 18–22. 5 p.

Pettissalo, S., Sauna-aho, S. Hänninen, S. & Lehtonen, M. 2000. A novel application for fault location in distribution networks. Proceedings of Southern African Power System Protection Conference, Johannesburg, South Africa, 8.–9. November: ESKOM and TSI (Technology Services International). Pp. 117–121.

Phadke, A.G. & Thorp, J.S. 1990. Computer Relaying for Power Systems. England: Research Studies Press Ltd. 286 p.

Poll, J. 1981. Sternpunktverlagerung in gelöschten 110 kV-Netzen. Elektrizitäts-wirtschaft. Frankfurt: VDEW. Pp. 810–813. (Jg. 80, Heft 22.) ISSN 0013-5496

Poll, J. 1983. Auswertung der Störungsschreibraufzeichnungen von kurzzeitigen Erdschlüssen on kompensierten Netzen. Elektrizitätswirtschaft. Frankfurt: VDEW. Pp. 311–317. (Jg. 82, Heft 9.) ISSN 0013-5496

Poll, J. 1984. Löschung von Erdschlußlichtbögen. Elektrizitätswirtschaft. Frankfurt: VDEW. Pp. 322–327. (Jg. 83, Heft 7.) ISSN 0013-5496

Pundt, H. 1963. Untersuchungen der Ausgleichsvorgänge bei Erdschluss in Hochspannungsnetzen mit isoliertem Sternpunkt und induktiver Sternpunkt-erdung als Grundlage zur selektiven Erdschlusserfassung. TU Dresden. 167 p. + app. (Dissertation.)

Reason, J. 1994. Relay detects downed wires by fault-current harmonics. Electrical World. USA: Pp. 58–59. (Vol. 208, No. 12.) ISSN 0013-4457

Rioul, O. & Vetterli, M. 1991. Wavelets and signal processing. IEEE Signal Processing Magazine. New York, USA: IEEE. Pp. 14–38. (Vol. 8, No. 4, October.) ISBN 1053-5888

Roman, H. & Druml, G. 1999. Distance location of earth faults in compensated medium voltage networks. Proceedings of CIRED'99, 15th International Conference and Exhibition on Electricity Distribution, 1–4 June 1999, Nice, IEE, 5 p. (CD-ROM)

Russell, B.D. & Benner, C.L. 1995. Arcing fault detection for distribution feeders: Security assessment in long term field trials. IEEE Transactions on Power Delivery. Pp. 676–683. (Vol. 10, No. 2.) ISSN 0885-8977

Russell, B.D. & Chinchali, R.P. 1989. A digital signal processing algorithm for detecting arcing faults on power distribution feeders. IEEE Transactions on Power Delivery. USA: IEEE. Pp. 132–140. (Vol. 4, No. 1, January.) ISBN 0885-8977

Russell, B.D., Mehta, K. & Chinchali, R.P. 1988. An arching fault detection technique using low frequency current components – performance evaluation using recorded field data. IEEE Transaction on Power Delivery. USA. Pp. 1493–1500. (Vol. 3, No. 4.) ISBN 0885-8977

Schegner, P. 1989. Digitaler Erdschlssuniversalschutz. Konzept und erste Realisierung. Dissertation. Universität des Saarlandes Saarbrücken, Germany. 186 p.

Schrüfer, E. 1990. Signalverarbeitung. Numerische Verarbeitung digitaler Signale. Germany: Carl Hanser Verlag München Wien. 362 p. ISBN 3-446-15944-4

Shihab, S. & Wong, K.L. 2000. Detection of faulty components on power lines using radio frequency signatures and signal processing technigues. Proceedings of 2000 IEEE Power Society Winter Meeting. 23–27 January 2000. Singapore: IEEE. 4 p. (CD-ROM, 00CH37077C.) ISBN 0-7803-5938-0

Shiping, L. & Russell, B.D. 1991. Optimal arching fault detection using signal processing techniques. EPSR (Electric Power Systems Research). Switzerland: Pp. 121–128. (Vol. 21, No. 2.) ISBN 0378-7796

Sidhu, T.S., Singh, H. & Sachdev, M.S. 1995. Design, implementation and testing of an artificial neural networks based fault direction discriminator for protecting transmission lines. IEEE Transactions on Power Delivery. IEEE. Pp. 697–706. (Vol. 10, No. 2, April.) ISBN 0885-8977-95

Sultan, A.F., Swift, G.W. & Fedirchuk, D.J. 1992. Detection of hifh impedance arching faults using a multi-layer perceptron. IEEE Trancactions on Power Delivery. USA: IEE. Pp. 1871–1876. (Vol. 7, No. 4, October.) ISBN 0885-8677-92

Sultan, A.F., Swift, G.W. & Fedirchuk, D.J. 1994. Detecting arcing downed-wires using fault current flicker and half-cycle asymmetry. IEEE Transactions on Power Delivery. IEEE. Pp. 461–470. (Vol. 9, No. 1, January.) ISSN 0885-8977

Taimisto, S. 1993. Earth fault compensation in medium voltage distribution networks. Sähkö&Tele. Pp. 24–30. (Vol. 66, No. 1.) (In Finnish)

Taylor, H.M. & Karlin, S. 1984. An introduction to stochastic modeling. Orlando, USA: Academic Press Inc. 399 p. ISBN 0-12-684882-3

The Finnish Electricity Association Sener. 2000. Outage Statistics 1999. Helsinki, Sener. 21 p. (In Finnish)

Tungkanawanich, A., Abe, J., Kawasaki, Z.I. & Matsuura, K. 2000. Location of partial discharge source on distribution line by measuring emitted pulse-train electromagnetic waves. Proceedings of 2000 IEEE Power Engineering Society Winter Meeting. 23–27 January 2000, Singapore: IEEE. 6 p. (CD-ROM, 00CH37077C.) ISBN 0-7803-5938-0

Wai, D.C.T. & Yibin, X. 1998. A novel technique for high impedance fault identification. IEEE Transactions on Power Delivery. USA: IEEE. Pp. 738–744. (Vol. 13, No. 3, July.) ISSN 0885-8977

Warrington, A. R. van C. 1962. Protective relays, their theory and practice. Vol. 1. London: Chapman & Hall Ltd. 484 p.

Vaughan, M. & Moore, P.I. 2000. A non-intrusive power system arcing fault location system utilising the VLF radiated electromagnetic energy. Proceedings of 2000 IEEE Power Engineering Society Winter Meeting. 23–27 January 2000, Singapore: IEEE. 6 p. (CD-ROM, 00CH37077C.) ISBN 0-7803-5938-0

VDE 0228. 1987. Teil 2, Maßnahmen bei Beeinflussung von Fernmeldeanlagen durch Starkstromanlagen. Deutcshe Elektrotechnische Kommission im DIN und VDE (DKE).

Weiss, L.G. 1994. Wavelets and wideband correlation processing. IEEE Signal Processing Magazine. New York, USA: IEEE. Pp. 13–32. (Vol. 11, No. 1, January.) ISBN 1053-5888

Willheim, R. & Waters, M. 1956. Neutral earthing in high-voltage transmission. New York: Elsevier Publishing Co. 669 p.

Winter, K. 1988. Null point analysis – new method for detecting high resistance earth faults. ERA. Sweden: Pp. 18–20, 23–24. (Vol. 61, No. 5.) ISSN 0013-9939 (In Swedish)

Winter, K. 1993. Swedish distribution networks – A new method for earth fault protection in cable and overhead systems. DPSP'93. Fifth International Conference on developments in Power System Protection. Conference Publication No. 368, IEE. 4 p.

Xinzhou, D., Yaozhong, G. & Bingyin, X. 2000. Fault position relay based on current travelling waves and wavelets. Proceedings of 2000 IEEE Power Society Winter Meeting. 23–27 January 2000. Singapore: IEEE. 7 p. (CD-ROM, 00CH37077C.) ISBN 07803-5938-0

Yu, D.C. & Khan, S.H. 1994. An adaptive high and low impedance fault detection method. IEEE Transactions on Power Delivery. IEEE. Pp. 1812–1821. (Vol. 9, No. 4.) ISBN 0885-8977-94

Yu, I.K. & Song, Y.H. 1998. Wavelet analysis and neural network based adaptive singlepole autoreclosure scheme for EHV transmission systems. Electrical Power & Energy Systems. Great Britain: Elsevier Science Ltd. Pp. 465–474. (Vol. 20, No. 7.) ISBN 0142-0615-98

Published by

Vuorimiehentie 5, P.O.Box 2000, FIN–02044 VTT, Finland
Phone internat. +358 9 4561
Fax +358 9 456 4374

Series title, number and report code of publication

VTT Publications 453
VTT–PUBS–453

Author(s)
Hänninen, Seppo

Title

Single phase earth faults in high impedance grounded netwotrks

Characteristics, indication and location

Abstract

The subject of this thesis is the single phase earth fault in medium voltage distribution networks that are high impedance grounded. Networks are normally radially operated but partially meshed. First, the basic properties of high impedance grounded networks are discussed. Following this, the characteristics of earth faults in distribution networks are determined based on real case recordings. Exploiting these characteristics, new applications for earth fault indication and location are then developed.

The characteristics discussed are the clearing of earth faults, arc extinction, arcing faults, fault resistances and transients. Arcing faults made up at least half of all the disturbances, and they were especially predominant in the unearthed network. In the case of arcing faults, typical fault durations are outlined, and the overvoltages measured in different systems are analysed. In the unearthed systems, the maximum currents that allowed for autoextinction were small. Transients appeared in nearly all fault occurrences that caused the action of the circuit breaker. Fault resistances fell into two major categories, one where the fault resistances were below a few hundred ohms and the other where they were of the order of thousands of ohms.

Some faults can evolve gradually, for example faults caused by broken pin insulators, snow burden, downed conductor or tree contact. Using a novel application based on the neutral voltage and residual current analysis with the probabilistic method, it is possible to detect and locate resistive earth faults up to a resistance of 220 kΩ.

The main results were also to develop new applications of the transient based differential equation, wavelet and neural network methods for fault distance estimation. The performance of the artificial neural network methods was comparable to that of the conventional algorithms. It was also shown that the neural network, trained by the harmonic components of the neutral voltage transients, is applicable for earth fault distance computation. The benefit of this method is that only one measurement per primary transformer is needed. Regarding only the earth faults with very low fault resistance, the mean error in absolute terms was about 1.0 km for neural network methods and about 2.0 km for the conventional algorithms in staged field tests. The restriction of neural network methods is the huge training process needed because so many different parameters affect the amplitude and frequency of the transient signal. For practical use the conventional methods based on the faulty line impedance calculation proved to be more promising.

Keywords

power distribution, distribution networks, earth faults, detection, positioning, fault resistance, arching, neutral voltage, residual current, transients

Activity unit

VTT Energy, Energy Systems, Tekniikantie 4 C, P.O.Box 1606, FIN–02044 VTT, Finland

ISBN	Project number
951–38–5960–6 (soft back ed.) 951–38–5961–4 (URL: http://www.inf.vtt.fi/pdf/)	

Date	Language	Pages	Price
November 2001	English	78 p. + app. 61 p.	C

Name of project	Commissioned by

Series title and ISSN	Sold by
VTT Publications 1235–0621 (soft back ed.) 1455–0849 (URL: http://www.inf.vtt.fi/pdf/)	VTT Information Service P.O.Box 2000, FIN–02044 VTT, Finland Phone internat. +358 9 456 4404 Fax +358 9 456 4374